ORNL/TM-2006/53

Evaluation of ^{232}Th Neutron Resonance Parameters in the Energy Range 0 to 4 keV

October 2006

DOCUMENT AVAILABILITY

Reports produced after January 1, 1996, are generally available free via the U.S. Department Energy (DOE) Information Bridge.

Web site http://www.osti.gov/bridge

Reports produced before January 1, 1996, may be purchased by members of the public from the following source.

National Technical Information Service
5285 Port Royal Road
Springfield, VA 22161
Telephone 703-605-6000 (1-800-553-6847)
TDD 703-487-4639
Fax 703-605-6900
E-mail info@ntis.fedworld.gov
Web site http://www.ntis.gov/support/ordernowabout.htm

Reports are available to DOE employees, DOE contractors, Energy Technology Data Exchange (ETDE) representatives, and International Nuclear Information System (INIS) representatives from the following source.

Office of Scientific and Technical Information
P.O. Box 62
Oak Ridge, TN 37831
Telephone 865-576-8401
Fax 865-576-5728
E-mail reports@adonis.osti.gov
Web site http://www/osti.gov/contact.html

This report was prepared as an account of work sponsored by an agency of the United States Government. Neither the United States Government nor any agency thereof, nor any of their employees, makes any warranty, express or implied, or assumes any legal liability or responsibility for the accuracy, completeness, or usefulness or any information, apparatus, product, or process disclosed, or represents that its use would not infringe privately owned rights. Reference herein to any specific commercial product, process, or service by trade name, trademark, manufacturer, or otherwise, does not necessarily constitute or imply its endorsement, recommendation, or favoring by the United States Government or any agency thereof. The views and opinions of authors expressed herein do not necessarily state or reflect those of the United States Government or any agency thereof.

ORNL/TM-2006/53

Nuclear Science and Technology Division

EVALUATION OF ^{232}Th NEUTRON RESONANCE PARAMETERS IN THE ENERGY RANGE 0 to 4 keV

H. Derrien
L. C. Leal
N. M. Larson

October 2006

Prepared by
OAK RIDGE NATIONAL LABORATORY
P.O. Box 2008
Oak Ridge, Tennessee 37831-6285
managed by
UT-BATTELLE, LLC
for the
U.S. DEPARTMENT OF ENERGY
under contract DE-AC05-00OR22725

CONTENTS

	Page
LIST OF FIGURES	v
LIST OF TABLES	vii
ACRONYMS AND ABBREVIATIONS	ix
ACKNOWLEDGMENTS	xi
ABSTRACT	xiii
1. INTRODUCTION	1
2. THE EXPERIMENTAL DATABASE	1
3. CONDITIONS OF THE ANALYSIS	2
4 RESULTS OF THE ANALYSIS: THE NEUTRON TRANSMISSION AND CROSS SECTION DATA	5
5. RESULTS OF THE ANALYSIS: THE RESONANCE PARAMETERS	17
5.1 GENERALITIES	17
5.2 THE AVERAGE LEVEL SPACING AND NEUTRON STRENGTH FUNCTION REVISITED	19
5.3 THE RADIATIVE CAPTURE WIDTHS	23
5.4 THE RECOMMENDED AVERAGE RESONANCE PARAMETERS	24
6. THE COVARIANCE MATRICES OF THE RESONANCE PARAMETERS AND OF THE AVERAGE CROSS SECTIONS	27
7. CONCLUSIONS	29
8. REFERENCES	31

LIST OF FIGURES

Figure		Page
1	Experimental and calculated total cross sections in the thermal and low energy range	3
2	Experimental and calculated capture cross sections in the thermal and low energy range	3
3	Results of the SAMMY fits of the Olsen experimental transmission data in the energy range of 20 to 25 eV	6
4	Results of the SAMMY fit of Olsen experimental transmission data in the energy range of 50 to 80 eV	7
5	Results of the SAMMY analysis of the Olsen experimental transmission data in the energy range of 100 to 300 eV	8
6	Results of the SAMMY analysis of the Olsen experimental transmission data in the energy range of 500 to 750 eV	9
7	Results of the SAMMY analysis of the Olsen experimental transmission data in the energy range of 1500 to 1750 eV	10
8	Results of the SAMMY analysis of Olsen experimental transmission data in the energy range of 3000 to 3500 eV	11
9	Effective capture cross sections in the energy range of 150 to 240 eV	13
10	Effective capture cross sections in the energy range of 650 to 750 eV	13
11	Effective capture cross sections in the energy range of 1280 to 1410 eV	14
12	Effective capture cross section in the energy range of 2250 to 2400 eV	14
13	Effective capture cross sections in the energy range of 3800 to 4000 eV	15
14	Cumulative number of resonances in the neutron energy range of 0 to 4 keV	18
15	Differential distribution of the resonance spacings compared with the Wigner distribution	18
16	Differential distributions of the reduced neutron widths compared with the Porter-Thomas distributions	19

LIST OF FIGURES (continued)

Figure		Page
17	Integral distribution of the reduced neutron widths of the resonances having 99% of chance to be s-wave in the energy range of 0 to 2 keV (left side) and in the energy range 0 to 4 keV (right side)	20
18	Integral distribution of the p-wave resonance reduced neutron widths larger than 0.002 eV	22
19	The capture widths of the large s-wave resonances in the energy range below 1000 eV	26

LIST OF TABLES

Table		Page
1	Average experimental (1st) and calculated (2nd) neutron transmissions of Olsen ^{232}Th thickest samples	12
2	Average experimental and calculated effective capture cross sections	15
3	Average experimental capture cross sections compared with the present results	16
4	Local values of the s-wave neutron strength function	21
5	Local values of the p-wave neutron strength function	22
6	Average values of the radiative capture widths	23
7	The capture widths of the s-wave resonances in the energy range 0 to 1000 eV	25
8	Recommended values of averages resonance parameters	26
9	The resonance parameters in the neutron energy range 2.2 to 2.4 keV	28

ACRONYMS AND ABBREVIATIONS

at	atoms
b	barns (10^{-24} cm^{-24})
CERN	Conseil Europeen pour la Recherche Nucleaire
CLM	Crystal Lattice Model
ENDF/B	Evaluated Nuclear Data File
FGM	Free Gas Model
fm	fermic (10^{-24} cm)
GELINA	Geel Linear Accelerator
KURRI	Institute Kyoto University
ORELA	Oak Ridge Electron Linear Accelerator
ORNL	Oak Ridge National Laboratory
n-TOF	Neutron Time-of-Flight facility at CERN
RPI	Rensselaer Polytechnic Institute Linear Accelerator

ACKNOWLEDGMENTS

This work could not be performed without the help of P. Schillebeeckx, who made available the GELINA experimental capture data, and of F. Gunsing, who assisted in the interpretation of the n-TOF experimental resolution and normalization of the data. The authors wish to thank Royce Sayer for helpful discussions regarding use of the RSAP code and Joyce Echols for assistance with preparation of the document. A part of the evaluation was performed in the framework of a Coordinated Research Project (CRP) of the International Atomique Energy Agency (IAEA). This work was sponsored by the U.S. Department of Energy Nuclear Criticality Safety Program (NCSP) under contract DE-AC05-00OR22725 with UT-Battelle, LLC.

ABSTRACT

Neutron resonance parameters of ^{232}Th were obtained from the Reich-Moore SAMMY analysis of high-resolution neutron transmission measurements performed at the Oak Ridge Electron Linear Accelerator (ORELA) by Olsen in 1981, along with the high-resolution neutron capture measurements performed recently at the Geel Linear Accelerator (GELINA, Belgium) by Schillebeeckx and at the nTOF facility (CERN, Switzerland) by Aerts. The ORELA data were analyzed previously by Olsen with the Breit-Wigner multilevel code SIOB, and the results were used in the ENDF/B-VI evaluation. In the new analysis of the Olsen neutron transmissions by the modern computer code SAMMY, better accuracy is obtained for the resonance parameters by including in the experimental data base the recent experimental neutron capture data. The experimental data base and the method of analysis are described in the report. The neutron transmissions and the capture cross sections calculated with the resonance parameters are compared to the experimental values. A description is given of the statistical properties of the resonance parameters. The new evaluation results in a decrease in the capture resonance integral and improves the prediction of integral thermal benchmarks.

1. INTRODUCTION

The most recent evaluation of the ^{232}Th resonance parameters was performed in 1982 by D. K. Olsen[1] for ENDF/B-VI. The evaluation was based on the parameters obtained from the analysis of transmission measurements performed by Olsen et al.,[2] Ribon,[3] and Rahn et al.[4] and of capture measurements performed by Forman et al.[5] and Macklin et al.,[6] with additional information taken from the evaluations made by Derrien,[7] and Keyworth and Moore.[8] The Olsen evaluation used a smooth background cross section to represent the contribution of the truncated external resonances and of the part of the capture cross section due to the missed p-wave resonances. His evaluation was not intended to be a comprehensive study. The aim of the present work is to complete the evaluation by using the more efficient computer code SAMMY[9] and by adding to the experimental data base the recent capture measurements performed at Geel Linear Accelerator (GELINA) by Schillebeeckx et al.[10] and at the neutron time-of-flight (n_TOF) facilities of the Conseil Europeen pour la Recherche Nucleaire (CERN) by Aerts et al.[11,12] The evaluations by Olsen, Derrien, and Keyworth and Moore were not performed from direct analysis of experimental neutron transmission or capture data but rather were the results of averaging existing sets of resonance parameters. In the present evaluation, the resonance parameters were obtained mainly from a sequential analysis of an experimental data base, including the neutron transmission data taken at the Oak Ridge Electron Accelerator (ORELA) by Olsen et al., GELINA neutron capture data, and n_TOF neutron capture data.

A brief description of the experimental data base is provided in Sect. 2, and the conditions of the analysis are outlined in Sect. 3. The neutron transmissions and the cross sections calculated with the evaluated resonance parameters are compared with the corresponding experimental data in Sect. 4, and the statistical properties of the resonances parameters are described in Sect. 5.

2. THE EXPERIMENTAL DATA BASE

Two independent series of transmission measurements were performed by Olsen et al. at ORELA. The first series of measurements were performed at the 22-m flight path in the neutron energy range 0.01 to 16 eV, with ^{232}Th metallic samples of thicknesses ranging from 0.0387 to 0.193 at/b. The second series were performed at the 40-m flight path in the neutron energy range of 10 to about 100 keV with ^{232}Th metallic samples of thicknesses ranging from 0.000161 to 0.193 at/b. The nominal resolution was better than 0.2 ns/m in the energy range above 1.3 keV, allowing separation of the s-wave resonances in the neutron energy range up to about 4 keV. The total cross section in the energy range 0.01 to 10 eV was obtained from the first series of measurements, with a systematic error estimated to be less than 0.3%. In the resonance region, Olsen estimated the systematic errors on the measured total cross section by comparing the average transmission from the different samples. Using this method, Olsen obtained an upper limit of 0.5, 1.0, and 5.0% of the average total or potential scattering values for the neutron energies 16, 447, and 3505 eV, respectively.

The GELINA capture measurements were performed at a 58.4-m flight path in the neutron energy range of 10 to about 100 keV with a nominal resolution of 0.6 ns/m in the energy range of 0.4 to 2.3 keV, and of 0.3 ns/m in the energy range of 2.3 to 6.0 keV. The thickness of the ^{232}Th sample was 0.00318 at/b. The n_TOF measurements were performed at a 185-m flight path in the neutron energy range of 1 ev to 1 MeV, with a nominal resolution of 6.2 ns at 8 eV and 0.2 ns at 5 keV. The thickness of the sample was 0.00411 at/b. Both GELINA and n_TOF effective capture cross sections could be normalized by using the

saturated resonances of the low energy part of the data. Both measurements have about the same energy resolution at 4-keV neutron energy.

Several other experimental results were considered for evaluation in the thermal and low-energy range: (1) Chrien et al.,[13] capture cross sections (1979); (2) Lundgren,[14] capture cross sections (1968); (3) Little et al.,[15] total cross sections (1981); and (4) Kobayashi et al.,[16] total cross sections (1984). The Chrien measurements were performed at the Brookhaven National Laboratory Fast Chopper spectrometer for incident neutron energy between 0.03 and 15 eV. They were normalized to the value of 7.41 b obtained by activation technique at 0.0253 eV. The Lundgren data were taken at the Stockholm R1 Reactor Fast Chopper for incident neutron energy between 0.1 and 3.4 eV. The Little total cross sections were obtained at the Rensselaer Polytechnic Institute Linear Accelerator (RPI) at the 26.7-m flight path for incident neutron energy between 0.006 and 18.6 eV with a systematic uncertainty less than 1%. The Kobayashi total cross sections were obtained at the 22.1-m flight path of the Research Reactor Institute Kyoto University (KURRI) Electron Linear Accelerator for incident neutron energy between 0.004 and 300 eV with a systematic uncertainty of about 1%. These experimental data are shown in Figs. 1 and 2. In the present evaluation, all the experimental capture data in the thermal region were re-normalized to 7.35 b at 0.0253 eV. The value 7.35 b was the result of the evaluation performed by Trkov.[17] The re-normalization of the thermal total cross section was not needed since the experimental data of Olsen, Little, and Kobayashi were the results of absolute measurements leading to cross sections with accuracy better than 1%. The discrepancy between the present evaluation and the experimental in Fig. 1 is discussed further in Sect. 4.

All the selected experimental transmissions or total cross sections were found to be mutually consistent and allowed the determination of the total cross section or of the average total cross sections with an accuracy better than 1% of the potential scattering value. Therefore, a consistent SAMMY fit of the transmission or total cross section data could be performed without, or with very small, background or normalization corrections. The situation is different for the experimental capture data. The GELINA and n_TOF data are effective capture cross sections obtained with different sample thicknesses. They cannot be directly compared due to different self-shielding and multiple scattering corrections. Moreover, the normalization of the experimental capture data and the evaluation of the experimental background are not straightforward. In general, the consistency of several sets of experimental capture cross sections cannot be obtained without normalization corrections and background adjustments on each set data. The capture cross section data of Chrien et al. and of Lundgren et al. in the thermal energy range were corrected for the self-shielding and multiple scattering effects by the authors of the experiments. They agree in shape in the energy range up to about 1-eV neutron energy but disagree at higher energy (see also Fig. 2).

3. CONDITIONS OF THE ANALYSIS

The analysis code SAMMY uses the Reich-Moore formalism to calculate the cross sections in the resolved resonance energy range and Bayes method to fit the experimental data. The fit of the experimental data base is performed sequentially, and the covariance matrix generated from the fit of a data set is used as input to fit the next data set. The calculated cross sections are modified by the Doppler and experimental resolution broadening, the self-shielding and the multiple scattering in the samples, the background, and the normalization corrections. The description of the normalization and background

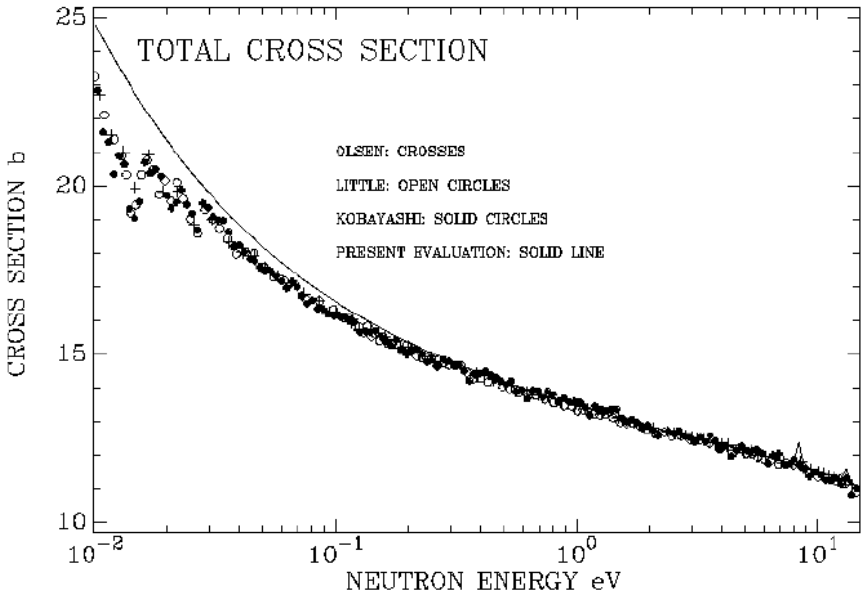

Fig. 1. **Experimental and calculated total cross sections in the thermal and low energy range.**

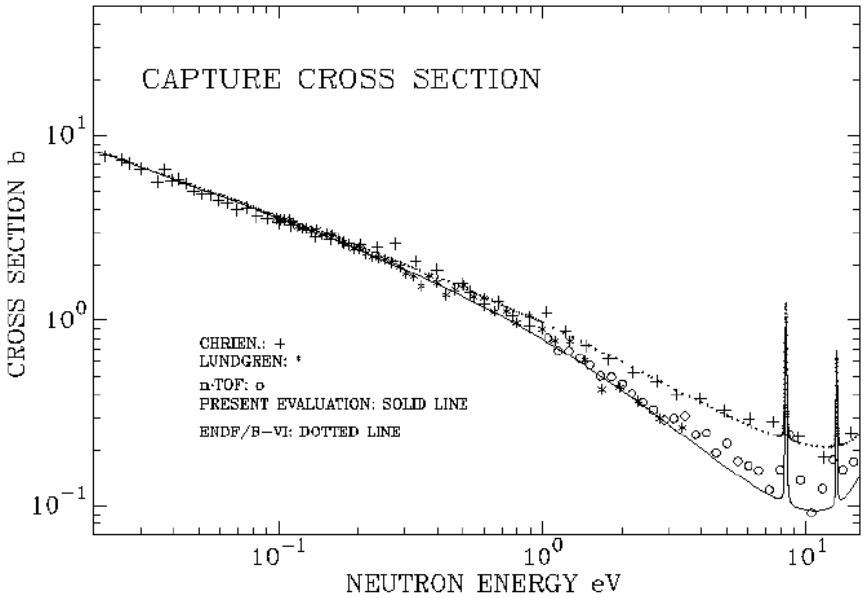

Fig. 2. **Experimental and calculated capture cross sections in the thermal and low energy range.**

evaluation is generally found in publications by the authors of the experiments, allowing the determination of reasonable correction parameters to be used as input in SAMMY. In case of inconsistent sets of experimental data, preliminary SAMMY runs could be useful for the evaluation of the correction parameters. The calculation of the multiple scattering in reaction cross section measurements is not straightforward and could be the source of important systematic errors found in published experimental capture cross sections. The method used in SAMMY for the calculation of the multiple scattering has been widely tested for the accuracy of the correction, particularly via the Monte-Carlo method.[18,19]

Doppler broadening of the resonances was calculated by the Free Gas Model (FGM) of Lamb.[20] Since all the experimental data analyzed were taken at room temperature with metallic samples, the value of 298 ± 5 K was used for the effective temperature of the samples. This value was obtained from a Debye temperature of 165 K recommended by Ribon.[3] The Crystal Lattice Model (CLM) is also available in SAMMY and could be more accurate for the analysis of the resonances at low energy where the Doppler broadening is predominant. The effects of the model on the determination of the parameters of the resonances at low energy were studied by several authors for the ^{238}U cross sections.[21–23] This effect was found to be very small for metallic samples at room temperature and is assumed to be negligible in the present analysis of ^{232}Th.

The usual components of the Time-Of-Flight (TOF) experimental resolution (i.e., the neutron burst width, the TOF channel width, and the uncertainties on the flight path length) were treated by the Gaussian-distribution option in SAMMY. The corresponding parameters are generally well known. Another part of the experimental resolution relates to the neutron slowing down and to the detectors (neutron detector or γ-ray detector). This part, which should be described by an asymmetrical function, is represented in SAMMY by the exponential $\exp(-t/\Delta t)$, where Δt is the so-called exponential folding width in microseconds (μs). The exponential folding width is not well known and could vary with the neutron energy. In the present evaluation, this parameter was obtained by preliminary fits of isolated resonances or group of resonances at different neutron energies for ORELA transmission and GELINA capture data. The n_TOF experimental resolution parameters were provided by Gunsing.[24] The channel widths of the n_TOF spectrometer at energy E vary smoothly as $E^{-1/2}$. The possibility of a channel width varying with energy was not available in the version of SAMMY used in the present evaluation. In the SAMMY n_TOF input file, the neutron energy range was divided into 22 energy intervals (E_i to E_{i+1}). For each energy interval, the channel width was equal to the exact value at the energy $(E_i+E_{i+1})/2$. The channel width at the edges of each interval had an error less than 10%.

The contribution of the resonances external to the energy range of 0 to 4 keV is important and is mainly due to the elastic scattering of the s-wave resonances. This contribution can be calculated from a set of resonance parameters obtained by translating a known set of resonances to the negative-energy region and to the region above 4 keV. This calculated contribution could then be fitted, with SAMMY, by few fictitious large resonances at negative energy and at energies above 4 keV. In the present evaluation, only two large fictitious resonances were used at -2 keV and +6 keV. Preliminary fits of the transmission data were performed without background and normalization corrections, in order to obtain the best value for the effective scattering radius R' and for the neutron width of the fictitious resonances at -2 and 6 keV. The value of 9.69 ± 0.03 fm was obtained for R', consistent with the value of 9.71 ± 0.08 obtained by Olsen from the analysis of the same experimental data,[2] the value of 9.65 ± 0.25 fm obtained by Kobayashi[25] from measured total cross section near 24 keV,[25] and the value of 9.65 ± 0.10 fm recommended by Ribon[3] from a resonance analysis of a thick-sample transmission data.

The analysis was started by using the ENDF/B-VI resonance parameters as prior values. This set of

parameters contained 241 s-wave resonances and 192 p-wave resonances in the neutron energy range of 0 to 4000 eV. The set of s-wave resonances could be considered as a complete set with an average level spacing of 16.6 eV. The set of p-wave resonances was far from complete since the average level spacing was 20.8 eV compared with 5.5 eV inferred from the s-wave average spacing. It is well known that missing the p-wave resonances has the effect of introducing an important bias in the calculated capture cross section. Olsen[1] has shown that the ^{232}Th resonance parameters that he evaluated for ENDF/B-VI, calculated average capture cross sections too small by a factor of 2 at 2 keV and by a factor of 4 at 4 keV, compared with the values calculated from a reasonable p-wave strength function. In the Olsen evaluation, the missing contribution was compensated by a smooth background cross section. To avoid the use of a background cross section in the present evaluation, a complete set of p-wave resonances was generated. This set, in addition to the p-wave resonances present in ENDF/B-VI and identified in the experimental neutron transmission and capture data, included fictitious resonances whose parameters were chosen at random in order to roughly comply with the Wigner distribution of level spacings and the Porter-Thomas distribution of reduced neutron widths with an average spacing of about 5.5 eV and a p-wave strength function about 1.6×10^{-4}. These resonances are too small to appear in the statistical fluctuations of the experimental data, or are hidden by the large resonances. This method of analysis was used previously for the ^{238}U resonance parameter evaluation in the energy range 0 to 20 keV.[23,26]

4. RESULTS OF THE ANALYSIS: THE NEUTRON TRANSMISSION AND CROSS SECTION DATA

Figures 1and 2 show the data in the thermal and low energy range. Below 0.1 eV, important deviations are observed between the calculated total cross section and the experimental values. Attempts to reproduce the average total cross section by negative energy resonance parameters in the energy range near 0.0253 eV have failed. In this energy range, all the experimental data are in good agreement. They show important structures due to the Bragg diffraction of neutrons. Extinction effects, which are microcrystalline effects, could cause a reduction of the coherent Bragg scattering and therefore a diminution of the measured total cross section. The calculated capture cross section at 0.0253 eV is 7.35 b, which is the value recommended by Trkov, and could be adjusted by small variations of the parameters of the fictitious resonance at -3.51 eV. In the energy range above 1 eV, the Chrien capture data are larger than those of Lundgren and n_TOF. The calculated cross section of the present evaluation follows the shape of Lundgren and n_TOF . The ENDF/B-VI evaluation follows the shape of Chrien; this agreement was obtained by Olsen by using a smooth background and not by the resonance parameters.

Figures 3 to 8 show examples of the SAMMY fits of the experimental transmission in the energy range of 20 to 3500 eV. The average values of the transmissions calculated from the resonance parameters are compared with some Olsen experimental data in Table 1. The agreements are generally better than 1.5% of the average transmission, corresponding to 0.06 b in the effective total cross section of the thickest sample, within the experimental error bars given by Olsen. Figures 3 to 8 also show excellent agreement in the pointwise representation of the experimental data.

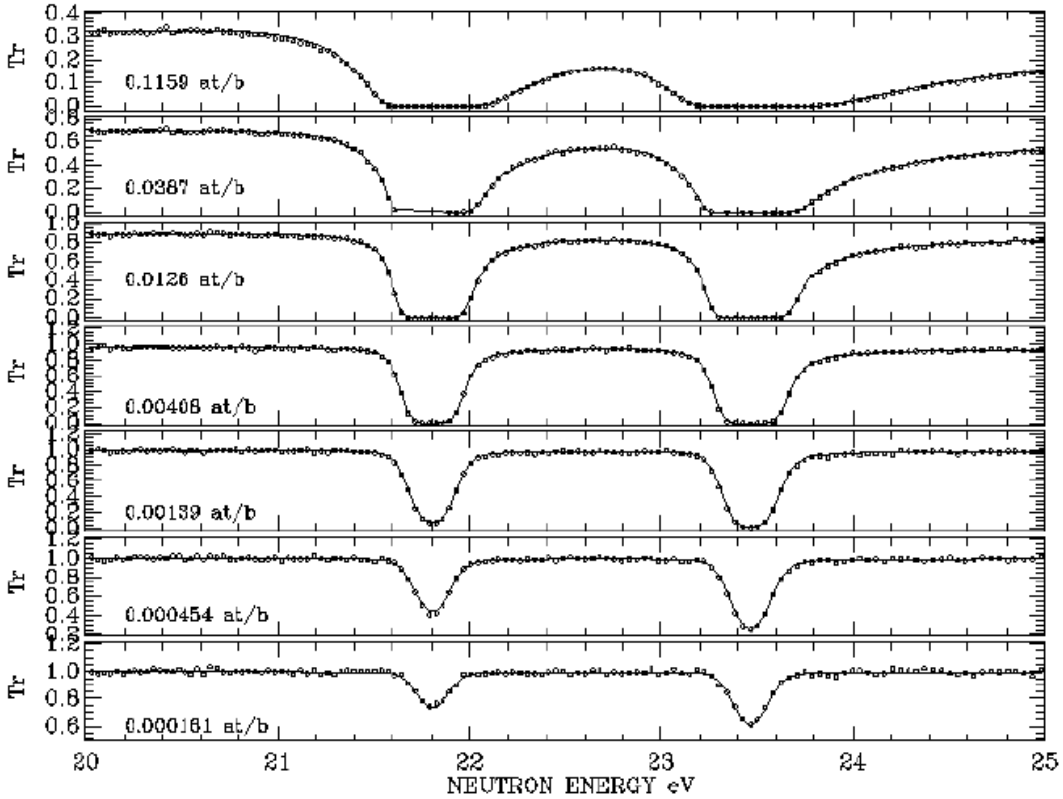

Fig. 3. **Results of the SAMMY fits of the Olsen experimental transmission data in the energy range of 20 to 25 eV.** The solid lines represent the neutron transmission calculated with the resonance parameters. The thickness of the sample is given with the corresponding data.

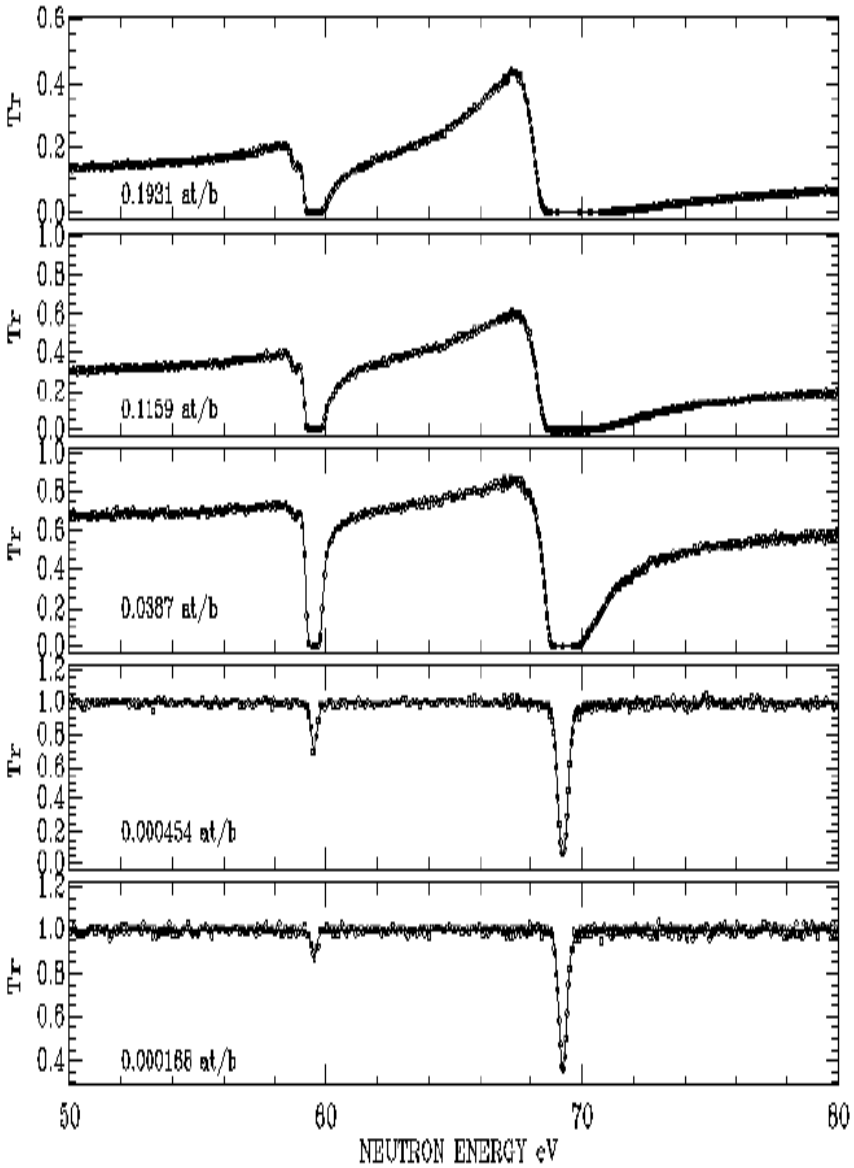

Fig. 4. **Results of the SAMMY fit of Olsen experimental transmission data in the energy range of 50 to 80 eV.** The solid lines represent the neutron transmission calculated with the resonance parameters. The thickness of the sample is given with the corresponding data.

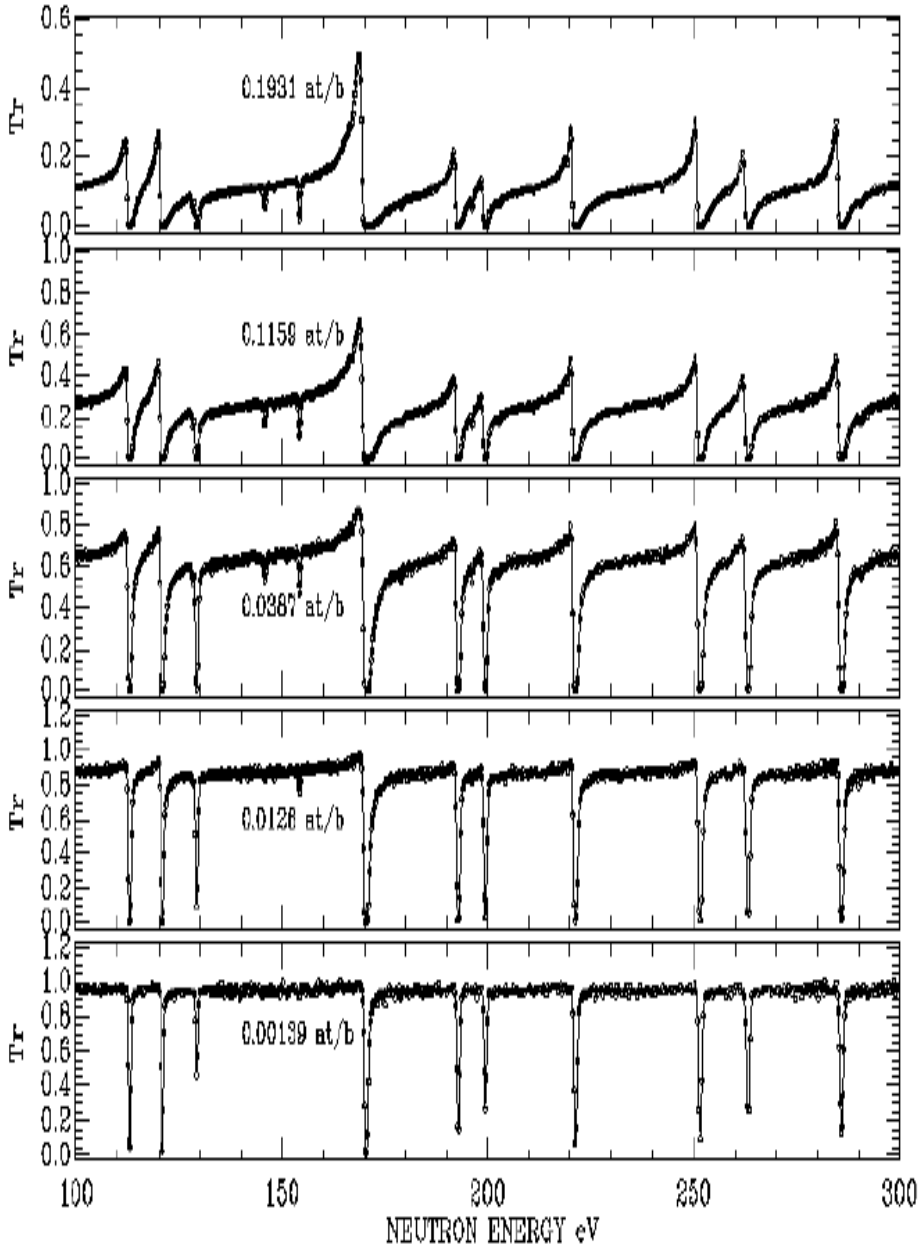

Fig. 5. **Results of the SAMMY analysis of the Olsen experimental transmission data in the energy range of 100 to 300 eV.** The solid lines represent the neutron transmission calculated with the resonance parameters. The thickness of the sample is given with the corresponding data.

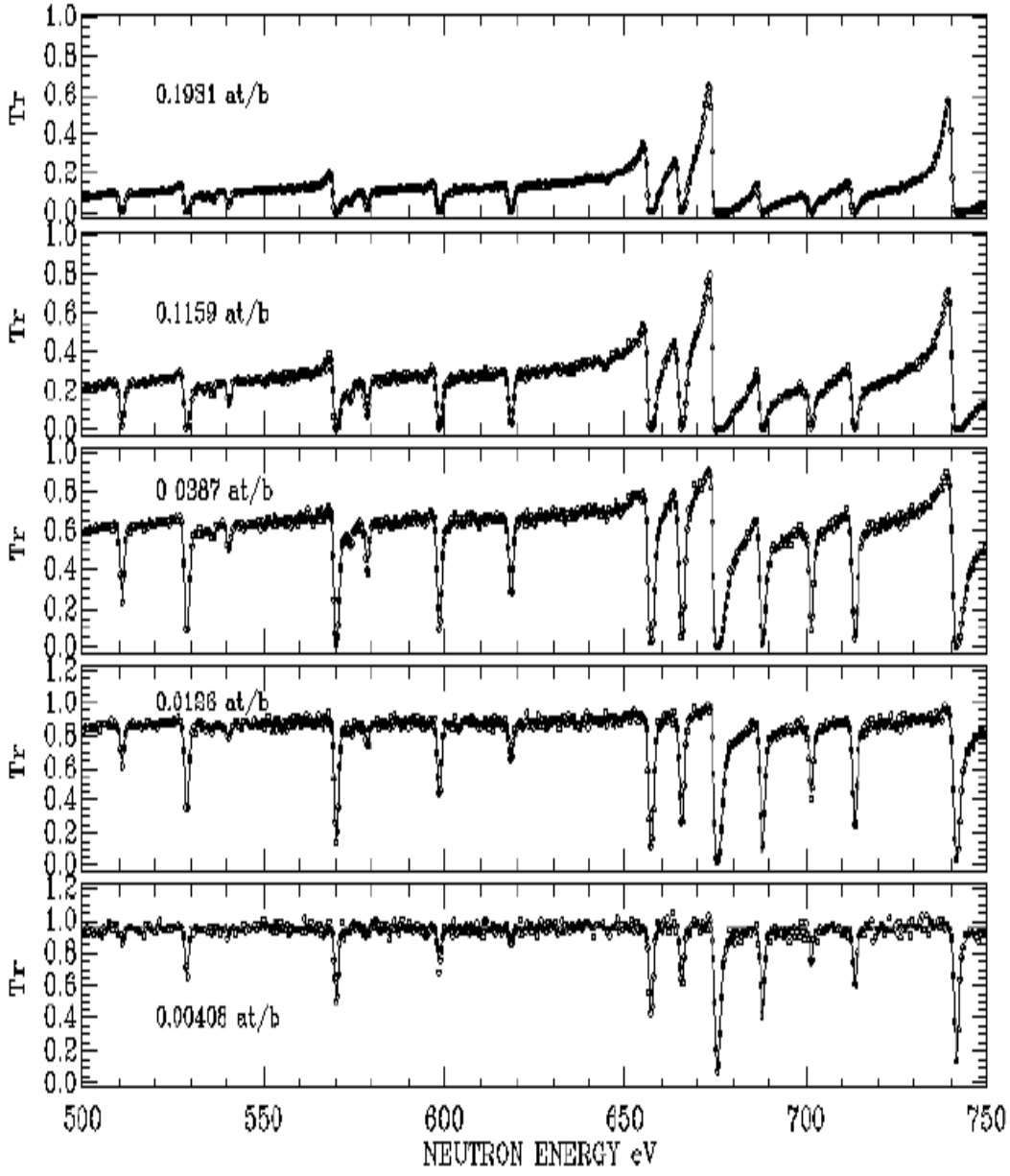

Fig. 6. **Results of the SAMMY analysis of the Olsen experimental transmission data in the energy range of 500 to 750 eV.** The solid lines represent the neutron transmission calculated with the resonance parameters. The thickness of the sample is given with the corresponding data.

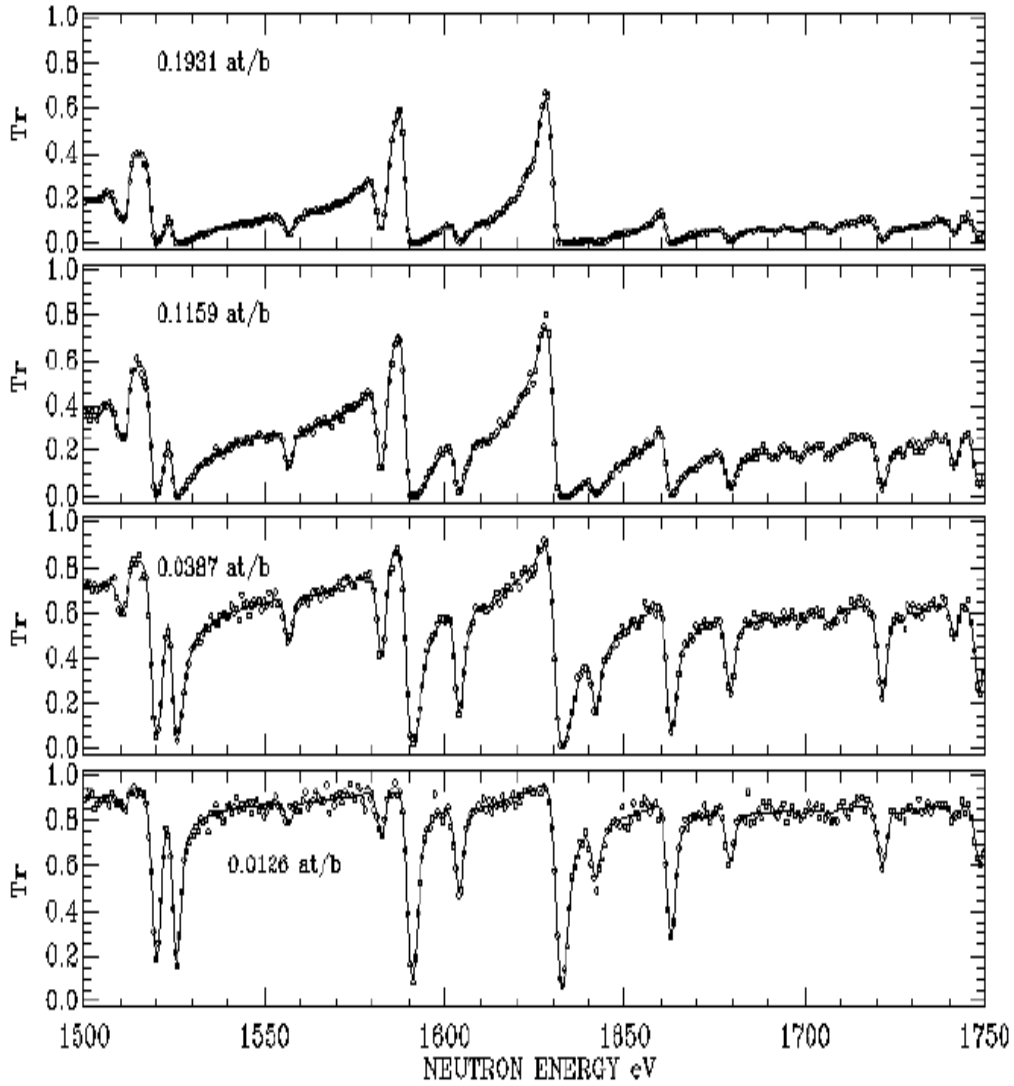

Fig. 7. **Results of the SAMMY analysis of the Olsen experimental transmission data in the energy range of 1500 to 1750 eV.** The solid lines represent the neutron transmission calculated with the resonance parameters. The thickness of the sample is given with the corresponding data.

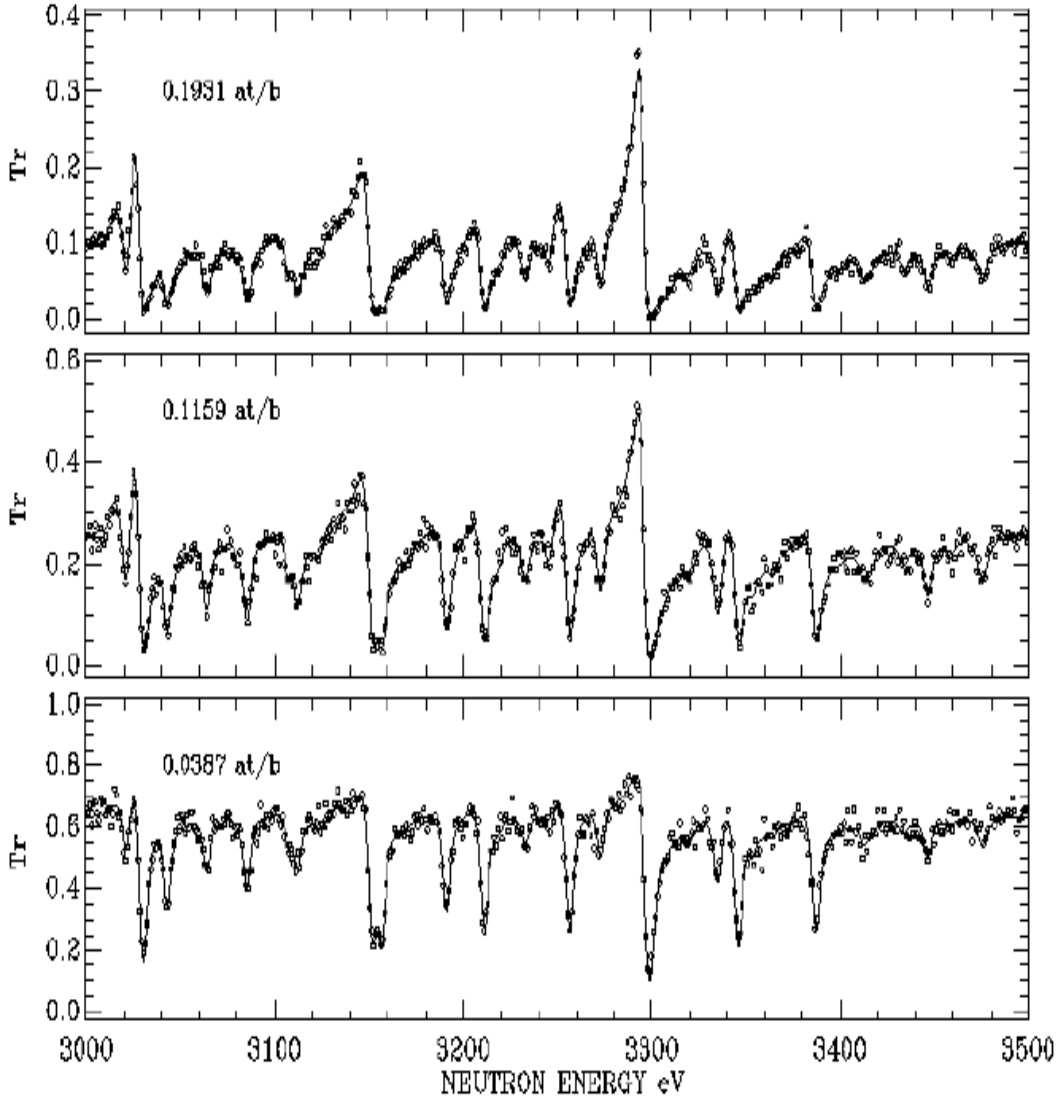

Fig. 8. **Results of the SAMMY analysis of Olsen experimental transmission data in the energy range of 3000 to 3500 eV.** The solid lines represent the neutron transmission calculated with the resonance parameters. The thickness of the sample is given with the corresponding data.

Table 1. Average experimental (1st) and calculated (2nd) neutron transmissions of Olsen ^{232}Th thickest samples

Energy range (eV)	Sample 0.0116 at/b			Sample 0.0387 at/b			Sample 0.193 at/b		
	1st	2nd	% deviation	1st	2nd	% deviation	1st	2nd	% deviation
20–50	0.601	0.602	0.06%	0.241	0.243	0.91%	0.099	0.1	1.00%
50–100	0.594	0.595	0.20%	0.25	0.251	0.40%	0.113	0.114	0.88%
100–500	0.466	0.465	-0.22%	0.188	0.188	0.00%	0.1	0.1	0.00%
500–1000	0.583	0.581	-0.34%	0.237	0.235	-0.85%	0.103	0.102	-1.00%
1000–1500	0.595	0.592	-0.51%	0.242	0.24	-0.83%	0.103	0.102	-1.00%
1500–2000	0.551	0.551	-0.00%	0.218	0.217	-0.46%	0.097	0.096	-1.00%
2000–2500	0.576	0.574	-0.35%	0.223	0.223	0.00%	0.092	0.091	-1.10%
2500–3000	0.545	0.546	0.18%	0.204	0.204	0.00%	0.085	0.084	-1.20%
3000–3500	0.565	0.564	-0.18%	0.207	0.208	0.48%	0.082	0.082	0.00%
3500–4000	0.582	0.58	-0.34%	0.22	0.218	-0.92%	0.086	0.086	0.00%
20–4000	0.573	0.571	-0.35%	0.223	0.223	-0.00%	0.094	0.093	-0.75%

Examples of SAMMY fits of the effective capture cross sections are shown in Figs. 9 to 13. The Geel experimental data were not normalized by the authors of the measurements. In the energy range above 200 eV, a good fit of the experimental data was obtained with a normalization coefficient of 6.80 ± 0.14 and a background correction of 0.35 ± 0.05 b. However the resonances at 21.80 and 23.46 eV needed a normalization coefficient of 7.09. The normalization coefficient decreased smoothly to 6.80 in the energy range of 20 to 200 eV. The background of 0.35 b represents 25% of the measured average cross section in the energy range of 3.5 to 4.0 keV.

No normalization adjustment was applied to the n-TOF data, and the background correction was very small (less than 0.5% of the average cross section in the energy range above 1 keV). The average effective capture cross sections calculated with the resonance parameters are compared with the corresponding experimental data in Table 2. The average capture cross sections were also obtained by Aerts et al.[11] and Gunsing[27] in the energy range above 1 keV from the same experimental data by using the computer code SESH[28] for the calculation of the self-shielding and multiple scattering corrections. When averaged over the energy range 1 to 4 keV, the Aerts results agree within 1% with the SAMMY calculation. However, when compared in energy intervals of 500 eV, differences of about ±5% are observed. These differences are due to the fact that the code SESH calculates the corrections from resonance parameters generated by the Monte-Carlo method, while SAMMY calculates the corrections from the current resonance parameters.

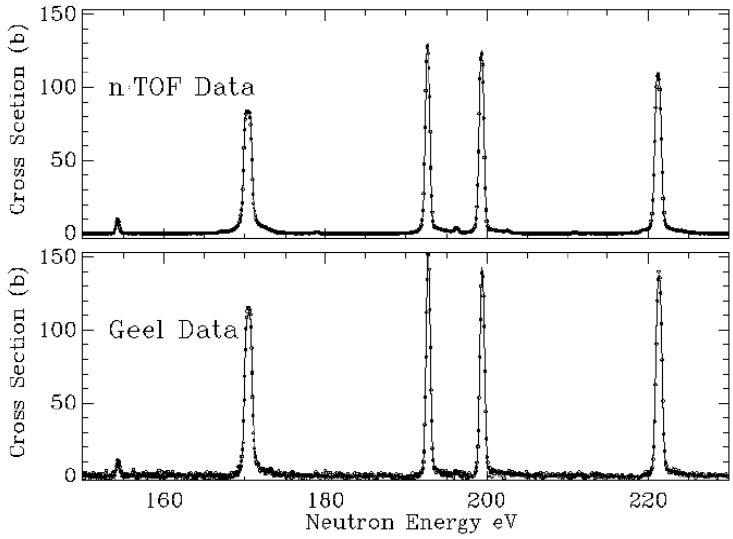

Fig. 9. Effective capture cross sections in the energy range of 150 to 240 eV. The solid lines represent the corresponding data calculated with the resonance parameters.

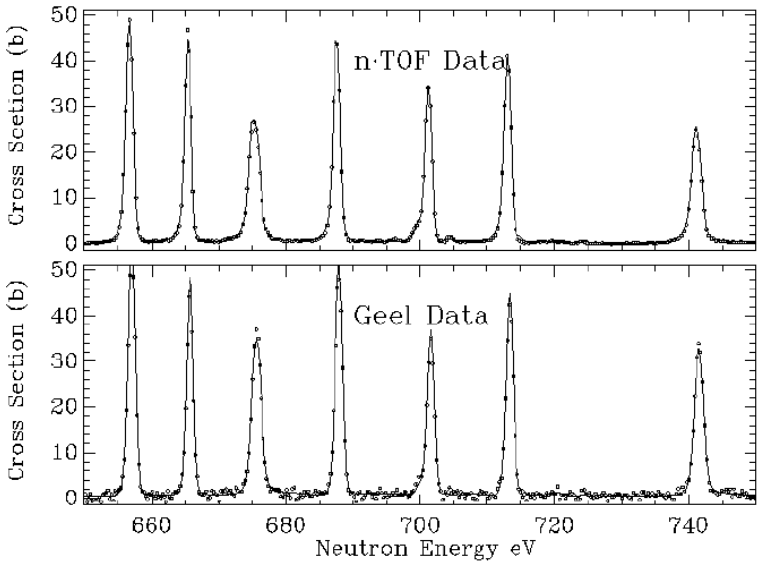

Fig. 10. Effective capture cross sections in the energy range of 650 to 750 eV. The solid lines represent the corresponding data calculated with the resonance parameters.

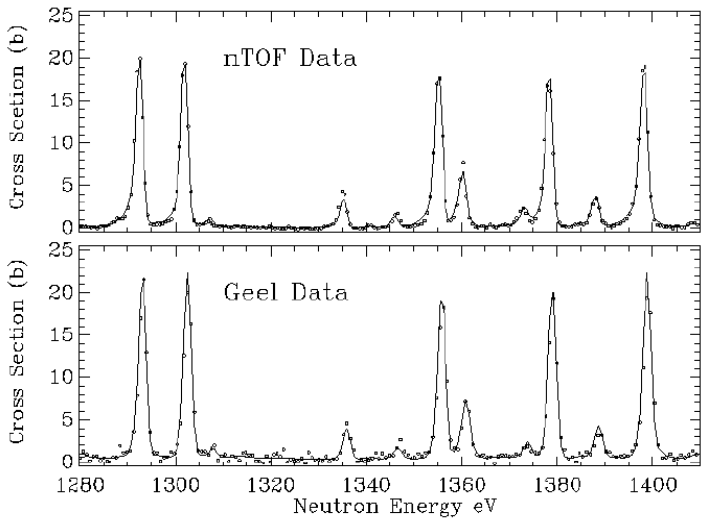

Fig. 11. **Effective capture cross sections in the energy range of 1280 to 1410 eV.** The solid lines represent the corresponding data calculated with the resonance parameters.

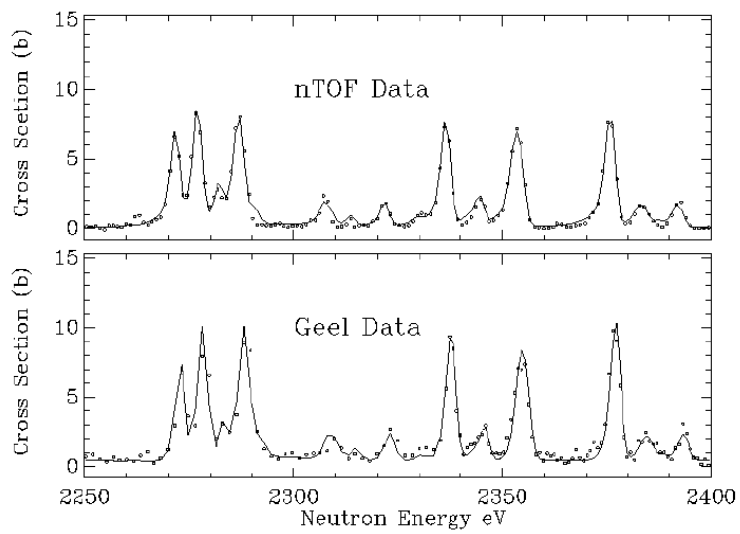

Fig. 12. **Effective capture cross section in the energy range of 2250 to 2400 eV.** The solid lines represent the corresponding data calculated with the resonance parameters.

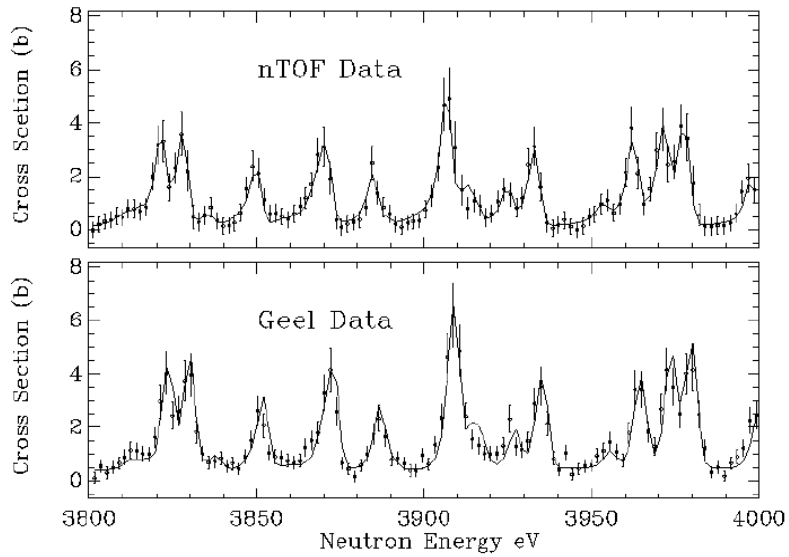

Fig. 13. **Effective capture cross sections in the energy range of 3800 to 4000 eV.** The solid lines represent the data calculated with the resonance parameters.

Table 2. Average experimental and calculated effective capture cross sections[a]

Energy range (eV)	Geel effective cross section			n-TOF effective cross section		
	Exp. (b)	Calc. (b)	Diff. (b)	Exp. (b)	Calc. (b)	Diff. (b)
20–50	7.65	8.86	1.21	7.316	7.486	0.17
50–100	6.09	6.37	0.28	5.357	5.478	0.121
100–500	5.19	5.38	0.19	4.627	4.487	-0.14
500–1000	2.9	2.62	-0.3	2.443	2.484	0.041
1000–1500	2.23	1.88	-0.35	1.817	1.805	-0.012
1500–2000	2.37	2	-0.37	1.946	1.931	-0.015
2000–2500	1.99	1.61	-0.36	1.557	1.563	0.006
2500–3000	1.9	1.56	-0.36	1.513	1.506	-0.01
3000–3500	1.63	1.27	-0.36	1.243	1.237	-0.01
3500–4000	1.45	1.1	-0.35	1.086	1.081	0.006

[a]The cross sections are given in barns. The last column contains the percentage deviation between ENDF/B-VI and the present evaluation.

Several results of average capture cross sections measurements are available in the energy range of 20 ev to 4 keV: Forman et al.[5], Chelnokov et al.[29], Macklin et al.[6], Kobayashi et al.[30], Grigoriev et al.[31] Large discrepancies are found among these experimental data. None of them agrees with the average capture cross section calculated from the resonance parameters of the present analysis. Some of the experimental results are compared with the present evaluation and to ENDF/B-VI values in Table 3. The most recent data are those obtained by Grigoriev et al., which show discrepancies as large as 50% when compared with the present evaluation. The percentage deviation between ENDF/B-VI and the present results increases from a few percent at low energy to about 10% on average at higher energy. A large part of the difference could be due to the method used by Olsen to evaluate the contribution of the missed p-wave resonance and will be examined in the next section.

The capture resonance integral calculated from the present evaluation is 82.34 b in the energy range of 0.5 ev to 4 keV, compared with the value of 83.62 b calculated from ENDF/B-VI. The contribution in the energy range of 4 kev to 20 MeV is 2.38 b from ENDF/B-V and ENDF/B-VI, which bring the present value to 84.72 b and ENDF/B-VI value to 86.00 b in the entire energy range of 0.5 ev to 20 MeV. Both results agree with the Greneche[32] evaluated value of 85.8 ± 1.9 b. Actually the new Oak Ridge National Laboratory (ORNL) evaluation is closer to the ENDF/B-V value of 84.00 b. The differences between the results come mainly from the contribution of the energy range of 0.10 to 10 eV where ENDF/B-V relied on Lundgren experimental data, ENDF/B-VI on Chrien data, and the new ORNL evaluation on Lundgren and n_TOF data.

Table 3. Average experimental capture cross sections compared with the present results[a]

Energy range	Gregoriev[31]	Forman[5]	Macklin[6]	ENDF/B-VI	Present	
21.5–46.5 eV	57.00			37.88	37.09	1.7%
46.5–100. eV	20.30			21.06	21.37	-1.5%
100.–215. eV	19.90			13.85	14.04	-1.4%
215.–465. eV	5.84			7.99	8.01	-0.3%
465.–1000. eV	3.96			3.35	3.2	4.5%
1000.–2150. eV	2.34			2.08	1.98	5.1%
2.0–3.0 keV		1.73		1.65	1.58	4.4%
3.0–4.0 keV		1.43		1.27	1.16	9.5%
2.75–3.00 keV			1.58	1.44	1.38	4.0%
3.00–3.25 keV			1.22	1.53	1.41	8.5%
3.25–3.50 keV			1.23	1.07	1.07	0.0%
3.50–3.75 keV			0.78	1.18	1.1	7.3%
3.75–4.00 keV			0.89	1.29	1.06	21.7%

[a]The cross sections are given in barns. The last column contains the percentage deviation between ENDF/B-VI and the present evaluation.

5. RESULTS OF THE ANALYSIS: THE RESONANCE PARAMETERS

5.1 GENERALITIES

The ^{232}Th nucleus has spin and parity $I^{\pi} = 0^{+}$. The neutron resonances are induced via one channel spin s = 1/2. The spin of the s-wave resonances (neutron of angular momentum l = 0) is $j^{\pi} = 1/2^{+}$, and the spins of the p-wave resonances (neutron of angular momentum l = 1) are $j^{\pi} = 1/2^{-}$ and $j^{\pi} = 3/2^{-}$. About 75% of the s-wave resonances can be easily identified in the experimental transmission data from the asymmetry due to the potential-resonant interference effect. The remaining s-wave resonances have reduced neutron widths smaller than 10% of the average value and must be discriminated against p-wave resonances. The p-wave neutron penetrability factor allows many p-wave resonances to be observed in the low-energy region of the experimental data. In the ENDF/B-VI evaluation, 79 p-wave resonances are reported in the energy range 0 to 1 keV, and only 17 in the energy range 3 to 4 keV. Actually, the increase of the Doppler and experimental resolution widths prevent the observation of emerging small resonances. They are hidden by the large s-wave resonances and contribute to a spurious enhancement of the s-wave strength function. This feature was ignored by the ENDF/B-VI evaluators, and the capture compensation for the missed p-wave resonances could have been overestimated.

The present evaluation uses 243 s-wave resonances and 667 p-wave resonances for the description of the cross sections in the energy range 0 to 4000 eV. In addition to the large fictitious resonances at -2 keV and 6 keV, which account for the far-off external resonances, a ladder of seven resonances at negative energies and of seven resonances in the energy range of 4.0 to 4.1 keV was used to help fit the data in thermal energy range and just below 4000 eV, respectively. The angular momentum assignments of the resonances seen in the experimental data were the same as those in ENDF/B-VI. These assignments were made by Keyworth and Moore[8] who used the experimental results[3,6,33] and adjusted the resulting assignments so that the s-wave population is consistent with the Δ_3 statistics of Dyson and Mehta.[34] Since no spin assignments were reported for the p-wave resonances, all the p-wave resonances were assumed to have $½^{-}$ spin in the ENDF/B-VI evaluation. In the present evaluation, 236 resonances have spin $½^{-}$, and 431 resonances have spin $3/2^{-}$. At the start of the evaluation, the p-wave spin assignments were chosen randomly with the two-spin-state population ratio of about 2. In some cases, the fit of the experimental capture data required re-assignment of the spin.

The statistical properties of the resonances parameters are illustrated in Figs. 14 to 16. Figure 14 shows the variation of the cumulative number of s-wave and p-wave resonances versus energy in the neutron energy range of 0 to 4 keV. The variation is nearly linear, with an average spacing of 16.5 eV for the s-wave resonances and of 6.00 eV for the p-wave resonances. According to the (2J+1) dependance of the level density, 9% of the p-wave resonances could still be missing, uniformly distributed in energy. Figure 15 shows the differential distributions of the level spacings compared with the corresponding Wigner distributions. The left side of the figure shows the data for the neutron energy range of 0 to 2 keV, and the right side shows the energy range of 0 to 4 keV. The experimental distributions agree reasonably well with the Wigner distributions. Figure 16 shows the differential distribution of the reduced neutron widths for the s-wave and p-wave resonances in the energy range of 0 to 2 keV (left side of the figure) and in the energy range of 0 to 4 keV (right side of the figure). The corresponding Porter-Thomas distributions are represented by the dashed histogram. The experimental data agree reasonably with the Porter-Thomas

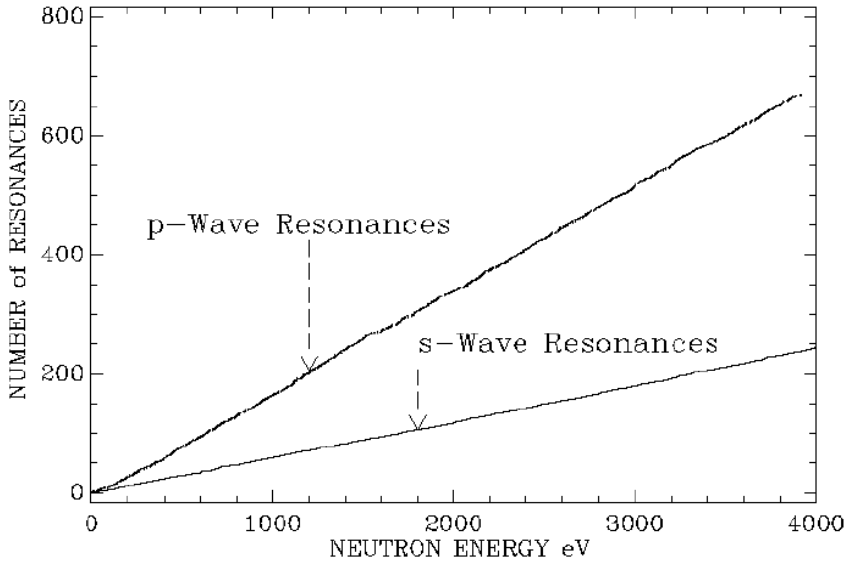

Fig. 14. Cumulative number of resonances in the neutron energy range 0 to keV.

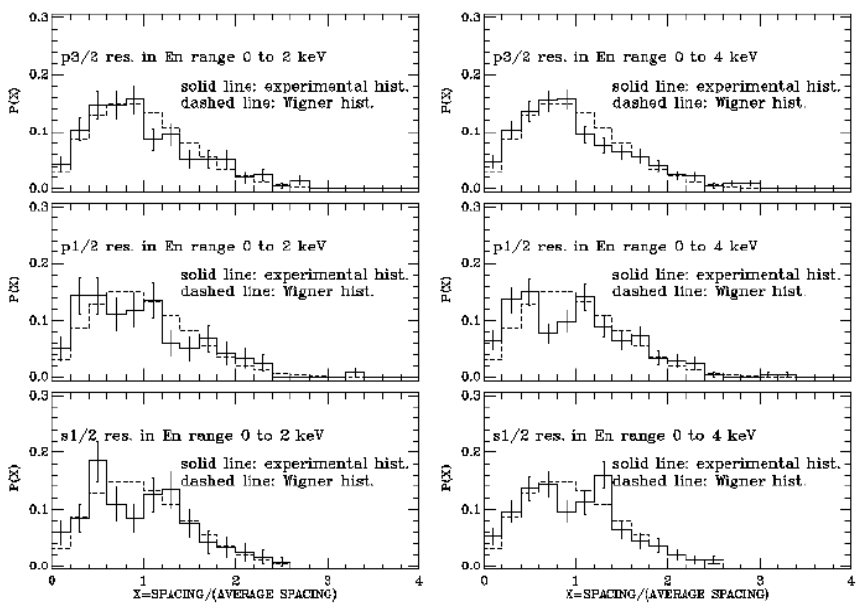

Fig. 15. Differential distribution of the resonance spacings compared with to the Wigner distribution.

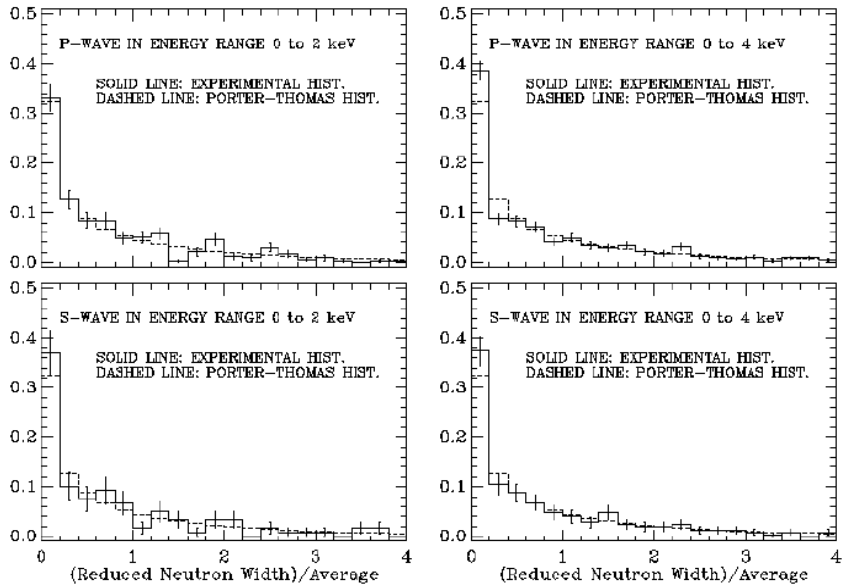

Fig. 16. Differential distributions of the reduced neutron widths compared to the Porter-Thomas distributions.

distributions. The set of resonances is nearly complete. This was achieved by adding to the resonances observed in the experimental neutron transmission and capture data, non-observed resonances whose energy and neutron widths were chosen to force the agreement with the Wigner and Porter-Thomas distributions. About 95% of the resonances assigned s-wave are seen in the experimental data, against 30% of the resonances assigned p-wave.

5.2 THE AVERAGE LEVEL SPACING AND NEUTRON STRENGTH FUNCTION REVISITED

The present comprehensive sequential SAMMY fit of the ORNL experimental transmission data and of the GEEL and n_TOF high-resolution capture data has achieved more accurate resonance parameters compared with the earlier evaluations, particularly in the high-energy region of the data. It is worthwhile to re-examine the properties of only those resonances seen in the experimental data in order to obtain an improved set of average parameters. Figure 17 shows the integral distributions of the observed resonances having 99% chance to be s-wave resonances. In the energy range of 0 to 2 keV, the distribution can be fitted by a Porter-Thomas distribution normalized to 123 resonances with an average reduced neutron width of 1.47 meV. The corresponding average spacing and strength function are 16.3 ± 0.5 eV and $(0.904 \pm 0.115)10^{-4}$, respectively. In the energy range of 0 to 4 keV, the distribution can be fitted by a Porter-Thomas distribution normalized to 242 values with an average reduced neutron width of 1.37 meV. The corresponding average spacing and strength function are 16.5 ± 0.3 eV and $(0.829 \pm 0.075)10^{-4}$, respectively.

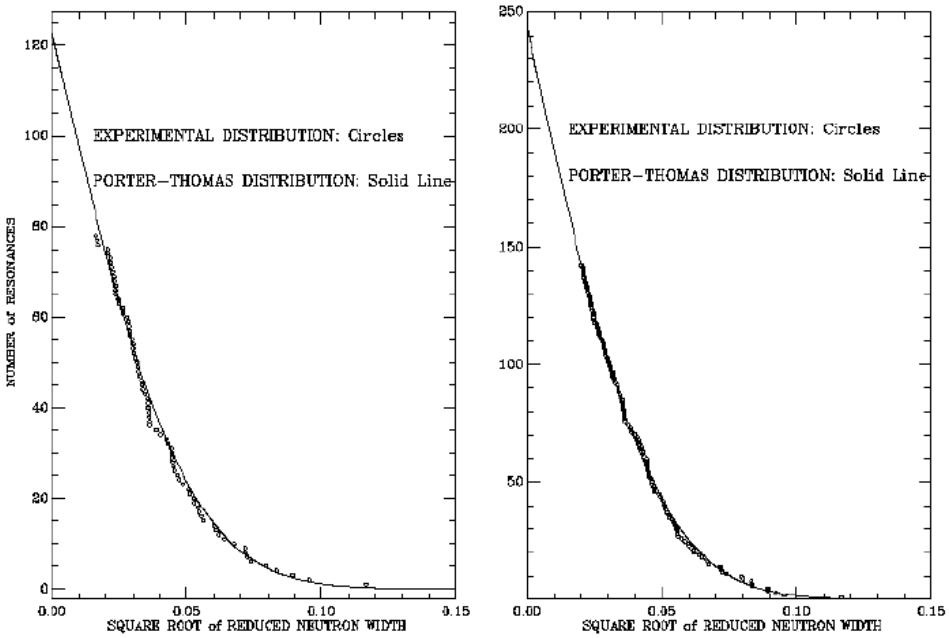

Fig. 17. Integral distribution of the reduced neutron widths of the resonances having 99% of chance to be s-wave in the energy range of 0 to 2 keV (left side) and in the energy range of 0 to 4 keV (right side).

The local values of the s-wave strength functions in 500-eV energy intervals obtained from the Olsen and Ribon resonance parameters are compared with the present values in Table 4. The values from Olsen and the present values should be in good agreement because they were obtained from the analysis of the same experimental data. Actually the agreement is quite good in the energy range below 1 keV, but the Olsen values are 5 to 6% larger in the energy range of 1 to 2 keV. The differences could be due to a different way of analyzing the experimental data. Olsen divided the experimental data into 15 energy intervals from 9 to 2030 eV with different contributions from the external resonances, while the present final analysis of each partial region was performed by using all the resonances of the region 0 to 4 keV with the same set of external resonance parameters. The Olsen s-wave neutron widths could also be slightly overestimated by the effect of the missing p-wave resonances. In the energy range of 0 to 3 keV, the strength function calculated from the Ribon parameters is 0.883×10^{-4}, which is in excellent agreement with the value of 0.894×10^{-4} calculated in the present evaluation in the same energy range. However, discrepancies of +6% and -9% are observed in the energy ranges 1 to 1.5 keV and 2.5 to 3.0 keV, respectively. Ribon obtained the resonance parameters from a Multi-Level Breit-Wigner least-square analysis of indirectly normalized thick-sample transmission data; his neutron widths were obtained with large error bars.

Table 4. Local values of the s-wave neutron strength function[a]

Energy range (keV)	Olsen[2]	Ribon[3]	ENDF/B-VI	Present
0.0–0.5	0.840 (1.1%)	0.862 (3.7%)	0.843 (1.4%)	0.831
0.5–1.0	0.815 (2.2%)	0.786 (-1.1%)	0.782 (-1.5%)	0.794
1.0–1.5	0.620 (6.2%)	0.634 (6.0%)	0.598 (2.4%)	0.584
1.5–2.0	1.347 (5.0%)	1.270 (-1.0%)	1.294 (0.9%)	1.283
2.0–2.5		0.706 (3.1%)	0.705 (2.9%)	0.685
2.5–3.0		1.037 (-9.0%)	1.145 (1.3%)	1.13
3.0–3.5			0.812 (8.1%)	0.751
3.5–4.0			0.513 (-9.0%)	0.559

[a]The percentage deviation with the present evaluation is given between parenthesis.

Figure 18 shows the integral distribution of the p-wave resonance reduced neutron widths $g\Gamma_n^1$ larger than 0.002 eV. Most of these resonances are seen in the experimental transmission or capture data, or have a significant contribution in the SAMMY fit of unresolved multiplets. The experimental distribution can be fitted by a Porter-Thomas distribution normalized to 725 ± 25 values with an average reduced neutron width of 0.00245 eV, which correspond to an average p-wave resonance spacing of (5.52 ± 0.20) eV and a p-wave strength function of $(1.48 \pm 0.15) \times 10^{-4}$. The average level spacing is consistent with the s-wave value inferred from Fig.17. The p-wave strength function was tentatively evaluated by Ribon[3] and by Corvi et al.[33] from their resonance parameters. Ribon obtained the value of $(1.4 \pm 0.5) \times 10^{-4}$ in the energy range of 0 to 500 eV. Corvi obtained the value of $(2.0 \pm 0.4) \times 10^{-4}$ in the energy range of 0 to 2000 eV from a set a 58 resonances with $g\Gamma_n^1$ larger than 0.2 meV, assuming that this set was complete, which is in contradiction to the present evaluation where more than 100 resonances have a $g\Gamma_n^1$ value larger than 0.2 meV in the energy range of 0 to 2000 eV.

The p-wave strength functions calculated from the present resonance parameters in energy intervals of 500 eV are compared with the corresponding ENDF/B-VI values in Table 5. The ENDF/B-VI values correspond to the observed p-wave resonances and are much smaller than the expected value of the strength function. Smooth cross sections were calculated by Olsen to compensate for this too-small-strength function. The present values take into account the observed resonances and the resonances introduced artificially to obtain agreement with the Wigner and Porter-Thomas distributions. The p-wave strength function calculated in the energy range of 0 to 4 keV is 1.429×10^{-4}, which is in agreement with the value inferred above from Fig. 18.

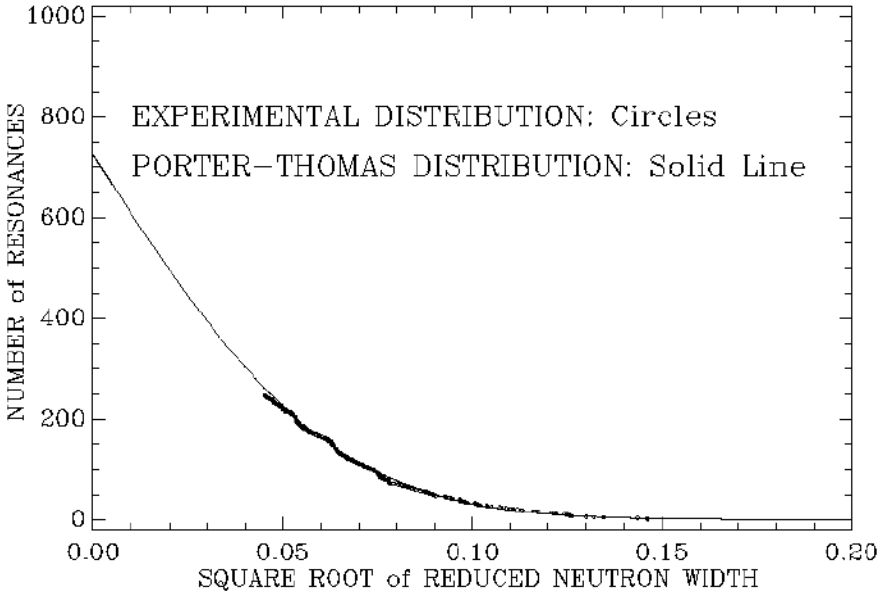

Fig. 18. **Integral distribution of the p-wave resonance reduced neutron widths larger than 0.002 eV.**

Table 5. Local values of the p-wave neutron strength function

Energy range (keV)	p-wave Strength function ($\times 10^4$) Present	ENDF/B-VI
0.0–0.5	1.193	0.898
0.5–1.0	1.206	1.018
1.0–1.5	1.237	0.93
1.5–2.0	1.433	0.794
2.0–2.5	1.588	0.736
2.5–3.0	1.662	0.739
3.0–3.5	1.862	0.538
3.5–4.0	1.209	0.496
0.0–4.0	1.429	0.768

5.3 THE RADIATIVE CAPTURE WIDTHS

Details on the radiative capture widths of the s-wave resonances obtained by several authors are found in the report by Olsen.[1] Two groups of average values have been recommended: one with values close to 21–22 meV (Ribon,[3] Rahn,[4] Forman[5] and Asghar[35]) and another with values close to 25 meV (Olsen[2], Macklin[6]). The values of 25.9 meV and 21 meV were adopted for ENDF/B-IV and ENDF/B-V, respectively. The average value adopted by Olsen for ENDF/B-VI was 24.4 ± 2.0 meV, evaluated from 17 resonances in the energy range of 20 to 350 eV. This value was used in the present evaluation as starting value for all the resonances in the SAMMY fits. Accurate values of the capture widths can be obtained from the shape analysis of transmission data only in the region where Doppler and resolution broadening is not too large compared with the total width of the resonances. The area of a resonance in the capture cross section is very sensitive to the capture width if the neutron width is larger, or of the same order of magnitude as the capture width. Therefore one should expect to obtain accurate values of the capture width for the large s-wave resonances from the SAMMY sequential analysis of the experimental transmission and capture data, even in regions where the Doppler and resolution broadening is important. This assumes that the multiple scattering effect is calculated with sufficient accuracy.

In the present evaluation, the capture width of the large s-wave resonances were allowed to vary in the SAMMY fits in all the energy ranges of the analysis. The average values of these capture widths, calculated by SAMMY, are given in Table 6 in energy intervals of 500 eV showing a tendency to decrease as the neutron energy increases. As shown in Table 2, these values allow a good reproduction of the average experimental capture data with a constant background correction of about 35 mb in the Geel data and a negligible correction in the n-TOF data, at least in the energy range above 1 keV. An attempt has been made to fit the experimental data by keeping the value of 24.4 meV for all the resonances. In this case, the effective capture cross sections calculated with the resonance parameters increase by 2–3%. The experimental data could not be fitted without an additional adjustment of the normalization. It is not clear whether the decrease of the average capture widths is due to an experimental effect in the measured cross sections. Further analysis is needed.

Table 6. Average values of the radiative capture widths

Energy range (keV)	Average capture width	Energy range (keV)	Average capture width
0.0–0.5	24.24 ± 0.04	2.0–2.5	22.78 ± 0.32
0.5–1.0	23.28 ± 0.14	2.5–3.0	22.75 ± 0.32
1.0–1.5	23.46 ± 0.29	3.0–3.5	22.36 ± 0.32
1.5–2.0	23.05 ± 0.26	3.5–4.0	25.47 ± 0.42

The values of the capture widths of the large s-wave resonances in the energy range 100 to 1000 eV are shown in Table 7. Three series of results are given in the table: the values obtained by Olsen from the SIOB[36] fit of the experimental transmission data; the values obtained in the present analysis from the SAMMY fit of the same transmission data; and the values obtained after the SAMMY analysis of all the experimental data (Olsen transmissions, Geel capture, nTOF capture, in this order in the sequential fit). The errors on the second and third series do not include the uncertainties on the Doppler and resolution broadening, and on the multiple scattering corrections. There is very good agreement between the SIOB values and the SAMMY values obtained from the analysis of the same experimental transmission data with different formalism and computer codes. The values obtained by fitting the transmission and the capture data base are on average smaller and have much smaller errors. Actually, when the neutron energy increases, the Doppler and resolution widths become much larger than the natural width of the resonances. Accurate values of the capture width cannot be obtained from the transmission data only. The capture widths of the large s-wave resonances are very sensitive to the capture area of the resonance, independently of the resolution. The adjustment of the capture width is obtained from the capture area with an accuracy depending mainly on the accuracy of the normalization and of the multiple scattering corrections in the capture data.

The capture widths of the energy range 0 to 1000 eV are plotted in Fig. 19. Above 400 eV the data show stronger fluctuations and the tendency to decrease is apparent. To avoid the effect of the systematic deviations, the average capture width should be evaluated in the energy range 0 to 400 eV only. The weighted average value calculated by SAMMY is 25.65 ± 0.10 meV from transmission data only and 25.24 ± 0.08 meV from transmission and capture data. These values compare to the value of 25.2 ± 0.5 meV obtained by Olsen from the transmissions in the same energy range and to the value of (24.4 ± 2.0) meV evaluated by Olsen for ENDF/B-VI.

5.4 THE RECOMMENDED AVERAGE RESONANCE PARAMETERS

Knowledge of the average resonance parameters is essential to the calculation of the neutron cross sections in the unresolved resonance energy range and at higher energy using statistical model or optical model. Analysis of the experimental data in these energy ranges by using the statistical or optical model is another way to obtain the average parameters. For example, the Hauser-Feshbach statistical model fit of the average experimental cross sections in the unresolved resonance energy range allows the determination of the neutron strength functions, the average partial widths, the nuclear radius, etc. However in general the fits are not unique because some of the parameters are strongly correlated. In the analysis of the resolved resonance region, the s-wave neutron strength function, the average reaction widths, and the effective scattering radius are generally obtained with good accuracy. These values used as input for a statistical model analysis of the unresolved energy range will allow more accuracy in the determination of the p-wave, d-wave, etc., average parameters.

Average parameters recommended from the present analysis are given in Table 8. The average level spacing and neutron strength functions come from the fit shown in Figs. 17 and 18. The effective scattering radius $R' = 9.69 \pm 0.03$ fm is the result of the fit of the Olsen thickest sample transmission data as explained in Sect. 3 of this report. The average radiative capture width is the value recommended from the analysis of the data in the energy range 0 to 400 eV.

Table 7. The capture widths of the s-wave resonances in the energy range 0 to 1000 eV

Energy (ev)	Olsen[2] SIOB[36]	Transmission only	Transmission and capture
21.809	25.3 ± 0.4	26.58 ± 0.11	26.48 ± 0.10
23.468	26.9 ± 0.4	27.40 ± 0.11	27.36 ± 0.10
59.530	24.6 ± 0.9	24.79 ± 0.20	24.49 ± 0.18
69.244	24.1 ± 0.3	24.23 ± 0.08	23.89 ± 0.07
113.055	26.1 ± 1.3	26.01 ± 0.23	25.80 ± 0.18
120.893	24.4 ± 0.6	24.70 ± 0.18	24.68 ± 0.14
129.214	27.5 ± 3.4	27.34 ± 0.91	28.11 ± 0.80
170.428	25.3 ± 0.6	26.39 ± 0.19	25.69 ± 0.14
192.761	25.8 ± 1.6	26.23 ± 0.50	25.14 ± 0.28
199.445	22.9 ± 2.6	24.01 ± 0.81	24.76 ± 0.44
221.330	26.1 ± 1.4	28.08 ± 0.42	26.22 ± 0.24
251.690	27.6 ± 1.5	28.37 ± 0.49	25.92 ± 0.26
263.279	23.9 ± 2.3	23.92 ± 0.72	23.89 ± 0.30
285.970	24.6 ± 2.0	24.36 ± 0.61	24.58 ± 0.29
305.690	25.1 ± 2.5	25.51 ± 0.74	24.68 ± 0.32
329.167	27.5 ± 1.5	26.49 ± 0.46	25.47 ± 0.28
342.068	26.7 ± 2.8	26.16 ± 0.84	23.08 ± 0.32
365.436	25.0 ± 4.0	24.14 ± 1.10	23.01 ± 0.36
369.566	24.0 ± 4.9	24.11 ± 1.32	24.30 ± 0.41
401.185		22.86 ± 1.82	23.82 ± 0.73
462.860		25.32 ± 0.86	24.50 ± 0.37
489.153		22.88 ± 1.00	23.84 ± 0.37
528.912		22.55 ± 2.01	22.62 ± 0.70
570.255		25.49 ± 1.82	22.78 ± 0.49
598.687		20.52 ± 1.98	20.81 ± 0.87
618.300		32.58 ± 2.91	30.52 ± 2.55
657.120		26.11 ± 1.63	24.50 ± 0.48
665.778		20.97 ± 1.85	22.18 ± 0.53
675.704		28.99 ± 0.92	24.72 ± 0.47
687.991		23.22 ± 1.83	23.00 ± 0.52
701.630		27.73 ± 2.62	24.51 ± 1.02
713.414		20.98 ± 1.96	21.97 ± 0.57
741.658		28.18 ± 0.73	24.34 ± 0.51
779.273		27.97 ± 0.25	27.49 ± 1.24
804.835		17.78 ± 0.77	21.42 ± 0.50
842.949		22.97 ± 0.41	23.44 ± 0.65
866.930		21.68 ± 2.11	23.30 ± 1.12
890.763		22.35 ± 2.11	23.06 ± 0.57
943.929		22.13 ± 2.12	23.55 ± 0.59
963.375		21.78 ± 2.19	20.75 ± 1.51
983.673		21.67 ± 2.22	25.12 ± 0.69
991.284		21.66 ± 1.88	23.67 ± 0.57

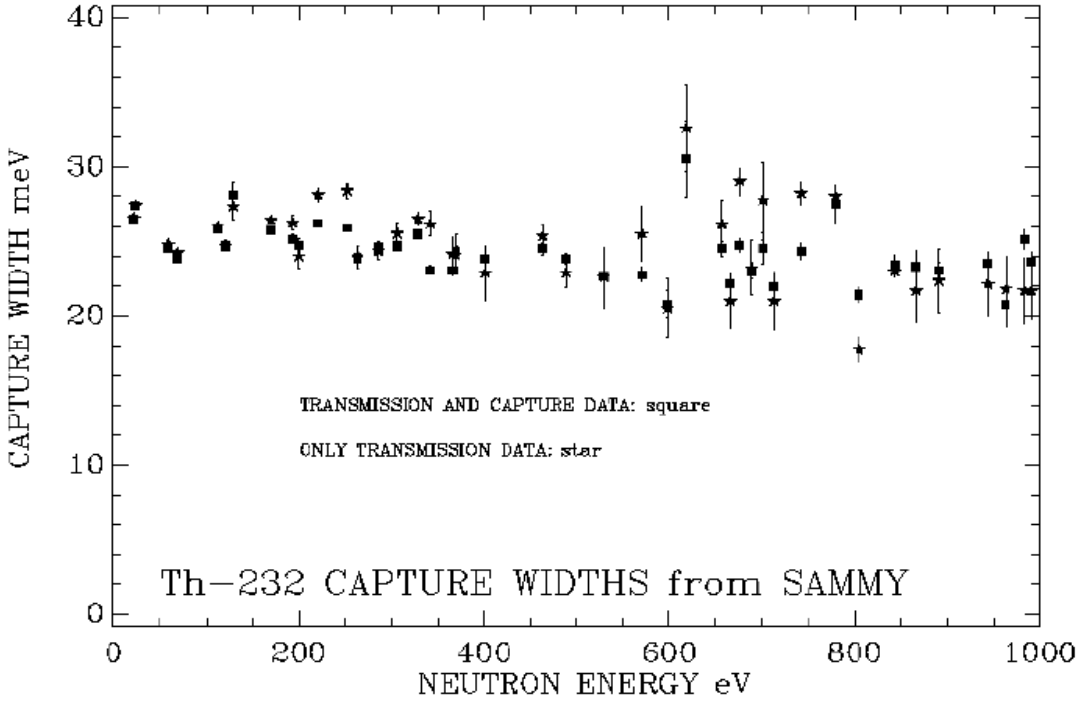

Fig. 19. The capture widths of the large s-wave resonances of the energy range below 1000 eV.

Table 8. Recommended values of average resonance parameters

	Average level spacing (eV)	Neutron strength function ($\times 10^4$)	Average capture width (meV)
s-wave	16.5 ± 0.3	0.829 ± 0.075	25.25 ± 1.00
p-wave	5.52 ± 0.20	1.48 + 0.15	

6. THE COVARIANCE MATRICES OF THE RESONANCE PARAMETERS AND OF THE AVERAGE CROSS SECTIONS

For the convenience of the analysis, the SAMMY fits were performed in partial energy ranges of 500 eV with iterations until reasonable accuracy was obtained on all the resonance parameters over the entire energy range of the analysis. This method allow the calculation of only partial covariance matrices. A complete SAMMY fit in the energy range 0 to 4000 eV should involve the search on more than 3600 resonance and experimental parameters, with an experimental data base of several hundred thousand data points. Even with the fastest computer, the calculation could last several days and will need several gigabytes of memories. These huge SAMMY calculations are feasible at ORNL by using the HP-Alpha computers in which 32 gigabytes of memories are available. A manageable parameter covariance matrix could be obtained in the entire energy range of the analysis by selecting the parameters which are the most important for the calculation of the group cross section errors and correlations, and by using the compact format proposed recently for the covariance files.[37] Nevertheless, these calculations could be performed only in the ultimate stage of the analysis by using as input a predetermined and final set of resonance and experimental parameters obtained from the more manageable partial energy range method as it is presented in this report. This ultimate stage of the analysis, which consists of building a complete covariance matrix, will be presented in another report.[38,39]

Examples of resonance parameters and errors obtained in the present evaluation in the energy range of 2.2 to 2.4 keV are provided in Table 9.

Table 9. The resonance parameters in the neutron energy range 2.2 to 2.4 keV

J	l	Energy (eV)	Energy error	Γ_γ (meV)	Γ_γ error	Γn (meV)	Γn error
0.5	0	2199.0259	0.0296	27.00	1.70	58.588	1.721
0.5	1	2201.6616	0.0266	24.40		3.528	0.268
1.5	1	2210.0000		24.40		1.000	
1.5	1	2207.0581		24.40		0.171	
0.5	1	2214.6951	0.0132	24.40		1.060	0.107
0.5	0	2217.9829	0.0063	16.82	1.36	28.936	1.028
1.5	1	2217.8711		24.40		0.012	
0.5	0	2223.6223	0.0115	23.46	1.47	97.521	2.012
0.5	0	2235.5259	0.0151	24.29	2.43	2.196	0.181
0.5	1	2235.6379		24.40		0.180	
1.5	1	2238.2117		24.40		0.243	
1.5	1	2248.0938		24.40		0.001	
1.5	1	2251.6309		24.40		0.001	
0.5	1	2259.2976		24.40		0.005	
1.5	1	2262.0000		24.40		0.080	
1.5	1	2265.7922		24.40		0.001	
0.5	0	2272.8528	0.0252	19.52	1.52	30.416	1.046
0.5	1	2276.2678		24.40		0.022	
0.5	0	2278.4685	0.0087	25.06	1.63	68.474	1.973
0.5	1	2284.1589	0.0126	24.40		4.150	0.258
0.5	0	2288.2637	0.0197	22.39	1.47	300.757	3.591
0.5	1	2292.7175	0.0109	24.40		0.738	0.074
1.5	1	2291.1055	0.0353	24.40		0.998	0.097
0.5	1	2296.7673		24.40		0.048	
1.5	1	2299.6838		24.40		0.070	
1.5	1	2307.5164	0.0040	24.40		1.104	0.102
1.5	1	2308.7893	0.0456	24.40		0.960	0.088
1.5	1	2313.6809		24.40		0.043	
1.5	1	2314.9915	0.0065	24.40		0.701	0.064
1.5	1	2322.5950		24.40		0.058	
0.5	0	2323.7739	0.0316	24.52	2.44	2.334	0.202
0.5	1	2322.7993	0.0069	24.40		1.471	0.137
1.5	1	2330.6038	0.0790	24.40		0.388	0.037
0.5	0	2337.8188	0.0257	21.29	1.23	124.037	2.374
1.5	1	2335.4846		24.40		0.052	
1.5	1	2343.6008	0.0319	24.40		0.415	0.039

7. CONCLUSIONS

The neutron resonance parameters of ^{232}Th were re-evaluated in the energy range of 0 to 4 keV from a Reich-Moore SAMMY analysis of the most recent experimental neutron transmission and neutron capture data. The experimental data base was formed mainly by the transmission measurements performed at ORELA by Olsen et al. in 1980, the effective capture cross section measurements performed at GELINA by Schillebeeckx et al. in 2002, and the effective capture cross section measurements performed at nTOF by Aerts et al. in 2003. The previous evaluation was performed by Olsen for ENDF/B-VI in 1981. The evaluation by Olsen was not intended to be a comprehensive study and used smooth background cross sections to compensate for the inadequacy of the resonance parameters to reproduce the totality of the cross sections. The present evaluation makes important improvements concerning the following points:

1. Two recent high-resolution effective capture cross section measurements (Geel and nTOF) were available for the present evaluation. By taking advantage of the ability of SAMMY to accurately calculate the multiple scattering effects in the thorium samples, we were able to calculate the average capture cross section to better than 3% accuracy.

2. In the energy range of 1.0 to 10 eV, the new resonance parameters reproduce the experimental capture cross sections inferred from the n-TOF measurements, in agreement with the early measurements of Lundgren. The ENDF/B-VI evaluation included a smooth cross section added to the contribution of the resonance parameters to obtain agreement with the measurements of Chrien et al. The capture cross section calculated in the present evaluation is about half as large as the ENDF/B-VI value and is closer to ENDF/B-V, which was based on Lundgren data in the energy range of 0.1 to 3 eV.

3. The contribution of the external resonances is fully represented by two fictitious resonances at -2 keV and 6 keV; in the ENDF/B-VI evaluation, this contribution was included as a smooth background cross section.

4. The present set of resonances is complete in that the statistical properties of the parameters agree with the Wigner distribution of the level spacings and with the Porter-Thomas distribution of the reduced neutron widths. This, particularly, allows the p-wave neutron capture cross section to be fully calculated with the resonance parameters. In the ENDF/B-VI evaluation, compensation for the missing p-wave resonances was calculated from the p-wave strength function and added as smooth background cross section.

5. Average resonance parameters obtained from the present evaluation confirm the ENDF/B-VI values with improved accuracy, particularly concerning the average capture width and the p-wave strength function.

8. REFERENCES

1. D. K. Olsen, *An Evaluation of the Resolved-Resonance-Region Cross Sections of ^{232}Th*, ORNL/TM-8056, ENDF-319, March 1982.

2. D. K. Olsen, R.W. Ingle, and J. L. Portney, "Measurement ad Resonance Analysis of the ^{232}Th Total Neutron Cross Section," *Nucl Sci. Eng.* **82**, 289 (1982).

3. P. Ribon, "Etudes de quelques proprietes des niveaux excites des noyaux composes formes par l'interaction de neutrons lents avc ^{103}Rh, Xe, ^{158}Gd, ^{232}Th," Thesis, C.N.R.S.A.3560, Orsay, France (January 1969); CEA-N-1149 (1969).

4. F. Rahn et al., "Neutron Resonance Spectroscopy.X. ^{232}Th and ^{238}U," *Phy. Rew.* **C6**, 1854 (1972).

5. L. Forman et al., "Th-232 Neutron Capture in the Region 20 eV-30 keV," p. 735 in *Neutron Cross Sections and Technology*, Vol. 2, Knoxville (1971).

6. R. L. Macklin and J. Halperin, *Nucl. Sci. Eng.* 64, 849 (1977), by R. L. Macklin in *Thorium Resonance Neutron Capture (2.6-10 keV)*, ORNL/TM-7732 (1981).

7. H. Derrien, "Evaluation of 232Th Resonance Parameters," p. 73 in *Specialist Meeting on Resonance Parameters of Fertile Nuclei and ^{239}Pu*, Paris, NEANDC(E)-163U, (1975).

8. G. A. Keyworth and M. S. Moore, "Cross Sections of the major Transactinium Isotopes in the Resonance Region," p. 241 in *Neutron Physics and Nuclear Data, Proc.of an Internat. Conf.*, Harwell (1978).

9. N. M. Larson, *Updated Users' Guide for SAMMY*, ORNL-9179/R6 and ENDF-364 (2003).

10. P. Schillebeeckx, private communication to L. C. Leal, Oak Ridge National Laboratory (2005).

11. G. Aerts et al., "Measurement of the ^{232}Th Neutron Capture Cross Section in the CERN n_TOF Facility," in *International Conference on Nuclear Data for Science and Technology*, Santa Fe, New Mexico, 20 Sept.–1 Oct. 2004, AIP Conference Proceedings 769 (2005).

12. G. Aerts et al., *The capture yield of the ^{232}Th(n,γ) measured at n-TOF-CERN, Internal Report*, DAPNIA-04-125 (May 19, 2004).

13. R. E. Chrien et al., "Neutron Cross Section of Thorium-232," *Nucl. Sci. Eng.* **72**, 202 (1979).

14. G. Lundgren, *Nukleonik* **11**, 51(1968).

15. R. C. Little, R. C. Block, and D. R. Harris, "Neutron Capture and Total Cross Section of Thorium-232 from 0.006 to 18 eV," *Nucl. Sci. Eng.* **79**, 175 (1981).

16. K. Kobayashi, Y. Fujita, and N. Yamamuro, "Neutron Total Cross Section Measurement of ^{232}Th in the off-resonance region below 300 eV," *Nucl. Sci. Eng.* **11** (7), 315 (1984).

17. A. Trkov, private communication to L. C. Leal, Oak Ridge National Laboratory (2005).

18. N. L. Larson and K. N. Volev, *Validation of Multiple Scattering Corrections in the Analysis Code SAMMY*, PHYSOR 2002, Seoul, Korea (October 7–10, 2002).

19. G. Noguere, "Measurements and Analysis of the I-127 an I-129 Neutron Capture Cross Sections," Ph.D. dissertation, CEA-R-6071 (2005).

20. W. E. Lamb, "Capture of Neutron by Atoms in a Crystal," *Phy. Rev.* **52**, 295 (1937).

21. A. Meister et al., "Experimental Study of the Doppler Broadening of Neutron Resonances at GELINA," pp. 435–439 in *Conference on Nuclear Data for Science and Technology*, Trieste, Italy, May 19–24, 1997 (1998).

22. D. Naberejnev, C. Mounier, and R. Sanchez, "The Influence of Crystalline Binding on Resonant Absorption," *Nucl. Sci. Eng.* **131**, 222–229 (1999).

23. H. Derrien et al., *Neutron Resonance Parameters of ^{238}U and the Calculated Cross Sections from the Reich-Moore Analysis of Experimental Data in the Neutron Energy Range from 0 keV to 20 keV*, ORNL/TM-2005/241 (2005).

24. F. Gunsing, private communication H. Derrien, Oak Ridge National Laboratory (2005).

25. K. Kobayashi et al., "Neutron Total Cross Section of Thorium Near 24 keV with an Iron-Filtered Neutron Beam," *Nucl. Sci. Eng*. **65**, 347 (1978).

26. M. G. Sowerby, Summary of the work of the NEANDC Task Force on U-238, NEANDC-313U (1994).

27. F. Gunsing, private communication to H. Derrien, Oak Ridge National Laboratory (2005).

28. F. H. Froehner, SESH, computer code, Report GA-8380 (1968).

29. V. B. Chelnokov et al., "Measurements of Radiative Capture and Fission Cross Sections for some Heavy Nuclei," *Atomnaya Energiya* **31**(2), 103 (1971).

30. K. Kobayashi, Y. Fujita, and N. Yamamuro, "Measurement of the Neutron Capture Cross Section of 232Th from 1 keV to 408 keV," *Nucl. Sci. Tech.* **18**, 823 (1981).

31. YU. V. Grigoriev et al., "Investigations of the ^{232}Th Neutron Cross Sections in the Resonance Energy Range," *Jadernye Konstanty*, YK-2000 (2), 3, Obninsk Report (January 2001).

32. D. Greneche, “Evaluation of the Th-232 Capture Resonance Integral,” *Proc. Specialist’ Meeting on Resonance Parameters of Fertile Nuclei and Pu-239,* Paris, May 20–22, 1974, NEANDC(E)-163U (1974).

33. R. Corvi, G. Pasquariello, and T. Van der Veen, “p-wave Assignment of ^{232}Th Neutron Resonances,” p. 712 in *Proceedings of an International Conference,* Harwell, September 1978, Organization for Economic Cooperation and Development (1978).

34. F. J. Dyson and M. L. Metha, *J. Math. Phys.* **4**, 703 (1963).

35. M. Asghar et al., “The Neutron Cross Sections of Thorium and the Analysis of the Resonances up to 1 keV,” *Nucl. Phys.* **76,** 196 (1966).

36. G. De Saussure, D. K. Olsen, and R. B. Perez, *SIOB: A Fortran Code for Least-Square Shape-Fitting of Several Transmission Measurements Using the Breit-Wigner Multilevel Formula,* ORNL/TM-6286, Oak Ridge National Laboratory (1978).

37. *ENDF-102, Data Format and Procedure for the Evaluated Nuclear Data File, ENDF-6,* written by the Members of the Cross Section Evaluation Working Group, ed. V. McLane, C. L. Dunford, and P. F. Rose, BNL-NCS-4495, Brookhaven National Laboratory (April 2001). Updated BNL-NCS-4495/04-Rev, ed. M. Herman (June 2005).

38. L. Leal et al., “Covariance Data for ^{232}Th in the Resolved Resonance Region,” *PHYSOR-2006,* Vancouver, Sept. 10–14, 2006.

39. G. Arbanas et al., “Covariance Data for 235U in the Resolved Resonance Region,” *PHYSOR-2006,* Vancouver, Sept. 10–14, 2006.

INTERNAL DISTRIBUTION

1. W. C. Carter, 5700, MS 6170
2. H. Derrien, 5700, MS 6171
3. M. E. Dunn, 5700, MS 6170
4. J. B. Echols, 5700, MS 6166
5. J. C. Gehin, 5700, 6712
6. N. M. Greene, 5700, MS 6171
7. K. H. Guber, 5700, 6171
8. J. O. Johnson, 5700, 6172
9. N. M. Larson, 5700, MS 6171
10. L. C. Leal, 5700, MS 6171
11. J. M. Norman, 4500N, MS 6227
12. C. V. Parks, 5700, MS 6170
13. J. E. Rushton, 4500N, 6243
14. R. O. Sayer, 5700, MS 6171
15. J. C. Wagner, 5700, MS 6170
16. R. M. Westfall, 5700, MS 6170
17. M. L. Williams, 5700, MS 6170
18. ORNL OTIC–RC, 6011, MS 6283

EXTERNAL DISTRIBUTION

19. F. A. Alpan, Westinghouse Electric Company, Nuclear Services, Mail Bin 18, P.O. Box 158, Madison, PA 15663 (alpanfa@westinghouse.com)
20. P. Blaise, DER/SPRC/LEPH, Batiment 230, Centre d'Etudes de CADARACHE, 13108 Saint Paul-lez-Durance, France
21. Olivier Bouland,CEA/DEN/DER/SPRG/LEPh, Cadarache Centre, F-13108 Saint-Paul-Lez-Durance Cedex, France
22. A. Brusegan, Central Bureau for Nuclear Measurements, Steenweg op Retie, 2240 Geel, Belgium
23. J. Burke, Gaerttner LINAC Laboratory Rensselaer Polytechnic Institute, Department of Environmental and Energy Engineering, Troy, NY 12180-3590
24. D. Cabrilla, U.S. Department of Energy, NE-40, 19901 Germantown Road, Germantown, MD 20874-1290
25. Allan D. Carlson, Ionizing Radiation Division, National Institute of Standard and Technology.
26. D. E. Carlson, U.S. Nuclear Regulatory Commission, Reactor and Plant System Branch, Division of System Research, Office of Nuclear Regulatory Research, MS T-10 G6, Rm. T-10, 17, Washington, DC 20555-0001
27. M. B. Chadwick, Los Alamos National Laboratory, MS B243 T-16, Los Alamos, NM 87545
28. J. Chang, Korea Atomic Energy Research Inst., Nuclear Data Evaluation Lab., P.O. Box 105, Yusang, Taejon 305-600, Korea
29. Arnauld Courcelle, CEA/DEN/DER/SPRG/LEPh, Cadarache Centre, F-13108 Saint-Paul-Lez-Durance Cedex, France
30. Patrick Cousinou, Institut de Radioprotection et de Surete Nucleaore, B.P. 17, 92262 Fontenay-aux-Roses, France

31. D. H. Crandall, NA-11/Forrestal Building, U.S. Department of Energy, 1000 Independence Ave., Washington, DC 20585

32. D. E. Cullen, Lawrence Livermore National Laboratory, MS-L-298, P.O. Box 808, Livermore, CA 94550

33. Y. Danon, Gaerttner LINAC Laboratory, Rensselaer Polytechnic Institute, Department of Environmental and Energy Engineering, Troy, NY 12180-3590

34. Jean-Pierre Delaroche, Department de Physique Theorique et Appliquee CEA/DAM, B.P. 12, F91680, Bruyere-Le Chatel, France

35. Emmeric Dupont, CEA/DEN/DER/SPRG/LEPh, Cadarache Centre, F-13108 Saint-Paul-Lez-Durance Cedex, France

36. J. R. Felty, Science Applications Intl. Corp., 2418 N. Dickerson St., Arlington, VA 22207

37. P. Finck, Argonne National Laboratory, Reactor Analysis Division, Bldg. 208, Argonne, IL 60439

38. S. C. Frankle, X-TM, MS B226, Los Alamos National Laboratory, Los Alamos, NM 87545

39. W. Furman, Frank Laboratory of Neutron Physics, JINR, Dubna, Russia

40. C. Gould, North Carolina State University, Physics Dept., Box 8202, Raleigh, NC 27695-8202

41. F. Gunsing, Centre D'Etudes De Saclay, F-Saclay - 91191, Gif-sur-Yvette Cedex, France

42. Robert Haight, Los Alamos National Laboratory, Los Alamos, NM 87545

43. A. Hasegawa, Nuclear Data Center, Japan Atomic Energy Research Institute, Tokai-mura, Naka-gun, Ibaraki-ken 319-11, Japan

44. M. Herman, National Nuclear Data Center, Bldg. 197D Brookhaven National Laboratory, Upton, NY 11973-5000

45. Tatania Ivanova, State Scientific Center of the Russian Federation, Institute for Physics and Power Engineering, Bondarenko Sq, Obninsk, Kaluga Region, 249020, Russian Federation

46. M. Jaeger, Inst. F. Strahlenphysik, Allmandring 3, Stuttgart D-70569, Germany

47. N. Janeva, Bulgarian Academy of Sciences, 72, Boul, Tzarigradsko shosse, Sofia 1784, Bulgaria

48. H. C. Johnson, U.S. Department of Energy, EM-21 Forrestal, 1000 Independence Ave., SW., Washington, DC 20585

49. Toshihiko Kawano, Los Alamos National Laboratory, MS B243, T-16, Los Alamos, NM 87545

50. Lambros Lois, U.S. Nuclear Regulatory Commission, 08 E23, 11555 Rockville Pike, Rockville, MD 20852-2746

51. G. Leinweber, Gaerttner LINAC Laboratory, Rensselaer Polytechnic Institute, Dept. of Environmental and Energy Engineering, Troy, NY 12180-3590

52. R. Little, Los Alamos National Laboratory, X-TM, MS B226, Los Alamos, NM 87545

53. M. Lubert, Gaerttner LINAC Laboratory, Rensselaer Polytechnic Institute, Department of Environmental and Energy Engineering, Troy, NY 12180-3590

54. C. Lubitz, Knolls Atomic Power Laboratory, P.O. Box 1072, Schenectady, NY 12301

55. R. E. MacFarlane, Los Alamos National Laboratory, T-2, MS B243, Los Alamos, NM 87545

56. Robert McBroom, U.S. Department of Energy, Oak Ridge Operations Office, 200 Administration Road, Oak Ridge, TN 37831

57. Jerry McKamy, EH-21 Germantown Building 270CC, U.S. Department of Energy, 1000 Independence Ave., SW, Washington, DC 20585-1290

58. Richard D. McKnight, Nuclear Engineering Division – Bldg. 208, Argonne National Laboratory, 9700 S. Cass Ave., Argonne, IL 60439

59. Russell D. Mosteller, Applied Physics Division, Los Alamos National Laboratory, NM 87545

60. C. Mounier, CEN Saclay, DMT/SERMA/LENR, 91191 Gif Sur Yvette Cedex, France

61. M. C. Moxon, 3 Hyde Copse, Marcham, Abingdon, Oxfordshire, England

62. S. F. Mughabghab, Brookhaven National Laboratory, Advanced Technology Building 197d, Upton, NY 11973-5000

63. Mark Nikolaev, State Scientific Center of the Russian Federation, Institute for Physics and Power Engineering, Bondarenko Sq, Obninsk, Kaluga Region, 249020, Russian Federation

64. C. Nordborg, OECD/NEA, Le Seine St-Germain 12, Boulevard des Iles, 92130, Issy-les-Moulineaux, France

65. P. Oblozinsky, National Nuclear Data Center, Bldg. 197D Brookhaven National Laboratory, Upton, NY 11973-5000

66. S. Y. Oh, Nuclear Data Evaluation Lab. Korea Atomic Energy Research Institute, P.O. Box 105, Yusung Taejon, 305-600 Korea

67. A. Plompen, Central Bureau for Nuclear Measurements, Steenweg op Retie, 2240 Geel, Belgium

68. A. Popov, Frank Laboratory of Neutron Physics, Joint Institute for Nuclear Research, RU-141980 Dubna, Moscow Region, Russia

69. C. Raepsaet, CEN Saclay, DMT/SERMA/LEPP, 91191, Gif Sur Yvette Cedex, France

70. Kevin Reynolds, U.S. Department of Energy, Oak Ridge Operations Office, 200 Administration Road, Oak Ridge, TN 37831

71. Pascal Romain, Department de Physique Theorique et Appliquee, CEA/DAM, B.P. 12, F91680, Bruyere-Le Chatel, France

72. Veronique Rouyer, Institut de Radioprotection et de Surete Nucleaire, BP 17, 92262 Fontenay-aux Roses, France

73. P. Rullhusen, Central Bureau for Nuclear Measurements, Steenweg op Retie, 2240 Geel, Belgium

74. P. Schillebeeckx, Central Bureau for Nuclear Measurements, Steenweg op Retie, 2240 Geel, Belgium

75. O. A. Shcherbakov, Petersburg Nuclear Physics Institute, 18 8 350 Gatchina, Leningrad District, Russia

76. R. Shelley, Central Bureau for Nuclear Measurements, Steenweg op Retie, 2240 Geel, Belgium

77. K. Shibata, Nuclar Data Center, Japan Atomic Energy Research Institute, Tokai-mura Naka-gun, Ibaraki-ken 319-11, Japan

78. R. Slovacek, Gaerttner LINAC Laboratory, Rensselaer Polytechnic Institute, Department of Environmental and Energy Engineering, Troy, NY 12180-3590

79. H. Takano, Nuclear Data Center, Japan Atomic Energy Research Institute, Tokai-mura, Naka-gun, Ibaraki-ken 319-11, Japan

80. M. A. Thompson, NA-117/Germantown Building GTN, U.S. Department of Energy, 1000 Independence Ave., SW, Washington, DC 20585-1290

81. Anatoly Tsiboulia, State Scientific Center of the Russian Federation, Institute for Physics and Power Engineering, Bondarenko Sq. Obninsk, Kaluga Region, 249020, Russian Federation

82. C. Wagemans, Central Bureau for Nuclear Measurements, Steenweg op Retie, 2240 Geel, Belgium

83. J. J. Wagschal, Racah Institute of Physics, The Hebrew University of Jerusalem, 91904, Jerusalem, ISRAEL

84. K. Yoo, Korea Atomic Energy Research Inst., Nuclear Data Evaluation Lab., P.O. Box 105, Yusung, Taejon 305-600, Korea

85. Phillip G. Young, Los Alamos National Laboratory, MS B243 T-16, Los Alamos, NM 87545